

| REPORT DOCUMENTATION PAGE | | | Form Approved OMB No. 0704-0188 | |
|---|---|--|---|--|
| <small>Public reporting burden for this collection of information is estimated to average 1 hour per response, including the time for reviewing instructions, searching existing data sources, gathering and maintaining the data needed, and completing and reviewing the collection of information. Send comments regarding this burden estimate or any other aspect of this collection of information, including suggestions for reducing this burden, to Washington Headquarters Services, Directorate for Information Operations and Reports, 1215 Jefferson Davis Highway, Suite 1204, Arlington, VA 22202-4302, and to the Office of Management and Budget, Paperwork Reduction Project (0704-0188), Washington, DC 20503.</small> | | | | |
| 1. AGENCY USE ONLY (Leave blank) | | 2. REPORT DATE April 1995 | | 3. REPORT TYPE AND DATES COVERED Final Report 10 Aug 94 - 10 Mar 95 |
| 4. TITLE AND SUBTITLE A Novel Instrumentation System for Measurement of Helicopter Rotor Motions and Loads Data | | | 5. FUNDING NUMBERS N00600-94-C-3087 | |
| 6. AUTHOR(S) Robert McKillip, Jr. | | | | |
| 7. PERFORMING ORGANIZATION NAME(S) AND ADDRESS(ES) Continuum Dynamics, Inc. P.O. Box 3073 Princeton, New Jersey 08543-3073 | | | 8. PERFORMING ORGANIZATION REPORT NUMBER | |
| 9. SPONSORING/MONITORING AGENCY NAME(S) AND ADDRESS(ES) NAWCAD/FTEG Patuxent River, Maryland 20670-5304 | | | 10. SPONSORING/MONITORING AGENCY REPORT NUMBER | |
| 11. SUPPLEMENTARY NOTES Dean Carico, Technical Monitor RW04B | | | | |
| 12a. DISTRIBUTION/AVAILABILITY STATEMENT UNCLASSIFIED - UNLIMITED | | | 12b. DISTRIBUTION CODE | |
| 13. ABSTRACT (Maximum 200 words) Results of a Phase-I SBIR study directed at a novel instrumentation system for the measurement of helicopter rotor motion and loads are described. Background into the requirements and needs of the measurement system are provided, along with a summary of past activities in this area. Consideration is then given to a novel scheme that incorporates blade-mounted accelerometer sensors with a simplified signal processing scheme to extract both rotor motion measurements, and to a limited extent, blade loading information. Issues regarding sensitivity of the system to modeling errors, nonlinearities and sensor bias errors are examined through detailed simulation and analysis. Also, a demonstration of the system performance for reconstructing flapping motion measurements is provided using Froude-scaled model rotor test results. Finally, implementation issues are discussed, and a plan for continued work leading to prototype development for this system is outlined. | | | | |
| 14. SUBJECT TERMS Rotor Instrumentation; Blade Motion; Accelerometer Sensors; Kinematic Observer; Helicopter Loads | | | 15. NUMBER OF PAGES 59 | |
| | | | 16. PRICE CODE | |
| 17. SECURITY CLASSIFICATION OF REPORT UNCLASSIFIED | 18. SECURITY CLASSIFICATION OF THIS PAGE UNCLASSIFIED | 19. SECURITY CLASSIFICATION OF ABSTRACT UNCLASSIFIED | 20. LIMITATION OF ABSTRACT UL | |

Phase I Final Report
For Period 10 August 1994 - 10 March 1995
Shipment No. SER0007Z
Item No. 0001AG
(Unclassified)



CONTINUUM DYNAMICS, INC.
P.O. Box 3073, Princeton, NJ 08543

19950413 068

DTIC QUALITY INSPECTED 6

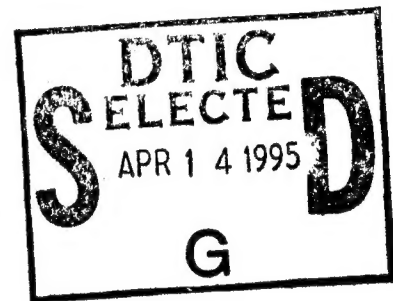
DISTRIBUTION STATEMENT A

Approved for public release;
Distribution Unlimited

SBIR Topic N93-283:
A Novel Instrumentation System for
Measurement of Helicopter Rotor Motions
and Loads Data

Phase I Final Report
For Period 10 August 1994 - 10 March 1995
Shipment No. SER0007Z
Item No. 0001AG
(Unclassified)

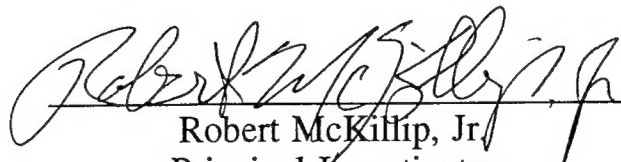
Prepared Under Contract No.
N00600-94-C-3087
for



Naval Air Warfare Center - Aircraft Division
Flight Test and Engineering Group, RW04B
Patuxent River, Maryland 20670-5304
Mr. Dean Carico, Technical Monitor

Prepared by

Continuum Dynamics, Inc.
PO Box 3073
Princeton, New Jersey 08543


Robert McKillip, Jr.
Principal Investigator
(609) 734-9282

10 April 1995

| | |
|--------------------------------------|---|
| Accession For | |
| NTIS | CRA&I <input checked="" type="checkbox"/> |
| DTIC | TAB <input type="checkbox"/> |
| Unannounced <input type="checkbox"/> | |
| Justification _____ | |
| By _____ | |
| Distribution / _____ | |
| Availability Codes | |
| Dist | Avail and/or Special |
| A-1 | |

DISTRIBUTION STATEMENT A

Approved for public release;
Distribution Unlimited

**Government Purpose License Rights
(SBIR Program)**

Contract No. N00600-94-C-3087

Contractor: Continuum Dynamics, Inc.

For a period of four (4) years after delivery and acceptance of the last deliverable item under the above contract, this technical data shall be subject to the restrictions contained in the definition of *Limited Rights* in DFARS clause at 252.227-7013. After the four-year period, the data shall be subject to the restrictions contained in the definition of *Government Purpose License Rights* in DFARS clause at 252.227-7013. The Government assumes no liability for unauthorized use or disclosure by others. This legend, together with the indications of the portions of the data which are subject to such limitations, shall be included on any reproduction hereof which contains any portions subject to such limitations and shall be honored only as long as the data continues to meet the definition on Government purpose license rights.

Copyright © 1995 Continuum Dynamics, Inc.
All Rights Reserved

A NOVEL INSTRUMENTATION SYSTEM FOR MEASUREMENT OF HELICOPTER ROTOR MOTIONS AND LOADS DATA

Robert M. McKillip, Jr.
Continuum Dynamics, Inc., Princeton, New Jersey 08543

SUMMARY

Results of a Phase-I SBIR study directed at a novel instrumentation system for the measurement of helicopter rotor motion and loads are described. Background into the requirements and needs of the measurement system are provided, along with a summary of past activities in this area. Consideration is then given to a novel scheme that incorporates blade-mounted accelerometer sensors with a simplified signal processing scheme to extract both rotor motion measurements, and to a limited extent, blade loading information. Issues regarding sensitivity of the system to modeling errors, nonlinearities and sensor bias errors are examined through detailed simulation and analysis. Also, a demonstration of the system performance for reconstructing flapping motion measurements is provided using Froude-scaled model rotor test results. Finally, implementation issues are discussed, and a plan for continued work leading to prototype development for this system is outlined.

TABLE OF CONTENTS

| | |
|---|-----|
| SUMMARY | iii |
| 1.0 INTRODUCTION AND BACKGROUND | 1 |
| 1.1 System Requirements | 2 |
| 1.2 Past Measurement Techniques | 2 |
| 1.3 Outline of Current Approach | 5 |
| 1.4 Phase-I Research Tasks and Final Report Outline | 10 |
| 2.0 SIMULATION DEVELOPMENT | 11 |
| 2.1 Transient Rotor Blade Simulation Features | 11 |
| 2.1.1 General | 11 |
| 2.1.2 Structural Model | 11 |
| 2.1.3 Aerodynamic Model | 11 |
| 2.1.4 Hub Loads Calculation | 12 |
| 2.1.5 Verification and Validation | 12 |
| 2.2 Simulation Goals Under Phase-I | 12 |
| 3.0 SIMULATION RESULTS | 13 |
| 3.1 Accuracy Assessment | 13 |
| 3.1.1 Instrumentation Requirements of the Methodology | 13 |
| 3.1.2 Demonstration on a Spring-Mass-Damper System | 14 |
| 3.1.3 Application to Flapping Motion Estimation | 16 |
| 3.1.4 Hardware Realization Implications | 20 |
| 3.2 Installation and Pre-Test Requirements | 22 |
| 3.3 Adjustment of Instrumentation System Bandwidth | 29 |
| 3.4 Sensitivity to Sensor Errors | 29 |
| 3.5 Self-Calibration and Self-Test | 30 |
| 3.6 Reconstruction of Rotor Loads | 30 |
| 4.0 HARDWARE DEMONSTRATION | 34 |
| 4.1 Description of Model Demonstration Hardware | 34 |
| 4.2 Scope of Tests | 36 |
| 4.3 Hover Response Comparisons | 37 |
| 5.0 IMPLEMENTATION ISSUES | 41 |
| 5.1 Sensor Technologies | 41 |
| 5.1.1 Optical Units | 41 |
| 5.1.2 Ultrasonic and Acoustic Units | 42 |
| 5.1.3 Magnetic Proximity Detectors | 42 |
| 5.1.4 Capacitive Probes | 42 |
| 5.1.6 RF Based Systems | 42 |
| 5.1.7 Inertial Measurement Units | 43 |
| 5.2 Signal Conditioning and Scaling | 44 |
| 5.3 Signal Transmission and Telemetry | 44 |
| 5.4 Signal Processing | 45 |
| 5.5 Data Storage and Archiving | 46 |
| 5.6 Instrumentation Power Issues | 46 |
| 5.7 Device Installation and Removal | 46 |
| 6.0 CONCLUSIONS FROM PHASE-I WORK | 48 |

TABLE OF CONTENTS (Cont'd)

| | |
|---|----|
| 7.0 PHASE-I OPTION WORK PLAN..... | 49 |
| 7.1 Hot-Bench Testing of System..... | 49 |
| 7.2 Telemetry and Power Conditioning Investigations | 49 |
| 8.0 RECOMMENDATIONS FOR PHASE-II CONTINUATION..... | 50 |
| 8.1 Extensions to Simulation Analysis..... | 50 |
| 8.2 Follow-On Demonstration Tests | 50 |
| 8.3 Device Prototyping | 50 |
| 9.0 REFERENCES | 51 |

1.0 INTRODUCTION AND BACKGROUND

U.S. Navy rotary-wing flight training and operational evaluation requirements have been aided through extensive use of manned flight simulators. These simulations can provide sufficient realism to reduce the number of operational flight hours required for flight and weapons system training, as well as provide scenarios and environmental factors that would be difficult or impossible to achieve on an as-needed basis (Ref. 1). With the ever-increasing computational capability in modern simulators, it has become possible to add additional realism by including more complicated physical models for the systems represented by the simulator's computers. However, if the added physics does not properly represent reality, the benefits of manned simulation may be lost due to having pilots interact with a representation that does not properly mimic the experience of actual flight trials. In such a situation, the personnel are being trained to operate the simulator and not the desired aircraft. In order to avoid this problem, high-fidelity flight simulators must be correlated against actual rotary-wing aircraft flight data. The ultimate goal of the effort described here would result in a simplified means of acquiring rotor motion and loads data, using a combination of accelerometer sensors and a Kinematic Observer processing structure, that would help the Navy to support this correlation exercise.

Rotorcraft simulation has progressed from simple adaptation of fixed-wing maneuvering flight models (Ref. 2) through early stability-derivative models (Ref. 3) and rotor map models (Ref. 4), to models that include both individual rotor blade motion (Ref. 5) and structural modes (Ref. 6). While this added modeling capability has been made easier by the steady improvement of computational performance, correspondingly significant advances have not been realized in the acquisition of supporting data to aid in the validation of this simulation software. This deficiency is primarily due to the difficulty in acquiring sensor data from helicopter rotor systems in general and isolated rotor blades in particular. Rotor blade instrumentation systems must operate in a severe dynamic environment, where centrifugal loads may range up to 900 g's at the rotor blade tip, and vibratory load spectra can extend out past 60 Hz on the main rotor. In addition, acquiring rotating-frame data necessitates the use of either on-blade telemetry or a slipping assembly for transmitting sensor input power and signal output to the fuselage or ground station for archiving. And finally, accommodating the particular geometric constraints of the rotor hub system may preclude convenient location of traditional motion sensing instrumentation.

While rotor motion and loads data has been collected for flight tests of helicopters for some time (Refs. 7-12), most of the instrumentation has required specialized blades, mounting hardware, or other significant modifications to the test aircraft. Although such compromises in implementation flexibility may be acceptable on a research aircraft, a truly useful helicopter rotor data acquisition system would avoid as many airframe-specific components as possible, thus allowing it to be used as a standardized piece of test equipment, much like an ordinary oscilloscope. The proposed instrumentation system under investigation in this Phase I effort would combine the convenience of using miniature accelerometer sensors, coupled to a Kinematic Observer signal processor, to provide rotor blade motion and loads data that approaches this ideal in aircraft application independence.

Development of the instrumentation approach described in detail in this report originated from a requirement to provide feedback signals to an Individual Blade Control (IBC) rotor system (Refs. 13, 14). Since each blade of an IBC rotor is controlled as an independent dynamic system, each must have sufficient on-blade sensors to provide a unique measurement or estimate of rotor blade modal responses. In order to satisfy this demand imposed by the control system design, blade-mounted accelerometers and strain

gauges were used in conjunction with a simplified signal processing scheme to produce accurate estimates of rotor blade modal displacements, velocities, and accelerations. Use of this processing scheme, referred to as a Kinematic Observer, allowed the implementation of a very simple control system structure due to the fact that estimation of the blade's response was not linked to any mathematical model of the rotor aerodynamics or equation of motion. This signal processing scheme combines the results of observer theory for dynamic systems with knowledge of the kinematic relationships between the sensors and the modal response of the blade structure. Details of the actual application of this methodology are given in a later section, but it is of interest to define the system requirements that guided the research effort conducted here under the Phase-I work. A summary of past methods and alternate current approaches in rotor system instrumentation follows, and then an outline of the report on the Phase-I work is presented at the end of this section.

1.1 System Requirements

As indicated in the preceding section, the ultimate goal of the research work described here is to provide a convenient means of acquiring helicopter (and, additionally, tiltrotor) rotor motion and loads data for use in correlation activities for improving manned flight simulators. The instrumentation should be capable of being conveniently installed on any rotary-wing aircraft in the Navy inventory, and provide accurate measurements of rotor motion and, to a limited extent, rotor loads, during flight operations in either a flight test or an actual training mission. The device should be compact and lightweight, so as not to interfere with the aerodynamic qualities of the rotor system or flying characteristics of the vehicle. It should not require excessive power, cabling, or signaling systems for support, and should be capable of being rapidly removed with no adverse impact on the original aircraft components. The instrumentation should also be robust, with sufficiently reliability to withstand the rigors of at-sea operation and not impose undue maintenance requirements on the flight engineer tasked with its installation. It should ideally be self-calibrating, and provide sufficient indications that a sub-component has failed and should be replaced. And finally, it should be easy to use, and interface readily with other Navy test instrumentation and data recording equipment.

While these goals may be laudable for any flight instrumentation equipment, they become a significant challenge for instrumentation that must operate in the dynamic environment of a modern rotor system on a helicopter or tiltrotor. Of primary importance is reliably collecting data across a rotating joint, with components capable of withstanding the inherent vibrations and centrifugal stresses that exist in and on the rotor blades themselves. Since direct electrical paths between the fuselage and the rotor system may not exist for a particular vehicle (such as through sliprings), the instrumentation must by nature be autonomous in terms of both its power supply and signal (data) transmission system. Thus, unattended operation for at least several hours is an absolute requirement if the unit is to maintain its usefulness.

Discussions of implementation issues for the proposed instrumentation system are postponed to a later section of this report. However, a more complete appreciation for the above requirements may be achieved after considering what is currently considered "state of the art" in this area of rotor instrumentation.

1.2 Past Measurement Techniques

As mentioned in the previous paragraphs, this effort would certainly not be the first attempt to measure rotor blade motion and loads for helicopters. Prior to the development of the transistor, back in the 1950's, the NACA mounted a high-speed movie camera on the hub of a helicopter to record the blade's bending and twisting motion as it spun about the

shaft. Later efforts in the early 1960's used strain-gauge technology and slip rings to measure blade bending moments, and pressure transducers were incorporated into research blades to record both chordwise and spanwise distributions of airloads. Reference 15 and 16 list a wide variety of rotor tests that have been conducted to measure rotor aerodynamic and structural loads and rotor motions.

Most of these past rotor instrumentation programs have been directed more toward aerodynamic measurements, with rotor motion and structural response measurements deemed a "secondary" set of data. Part of the reason for this focus has been the desire to achieve higher performance from the rotor aerodynamics through a more detailed understanding of the pressure distributions along the blade span and across the blade chords near the tip region. Another driving factor is the fact that, for older-technology rotor systems with small offset hinge locations, the net rotor forces may be approximated by only considering the aerodynamic loads, since the rotor blade inertial and structural loads effectively cancel at frequencies close to 1/rev. That is, the blade inertial flapping moment almost cancels the centrifugal moment at frequencies close to rotor rotation, so that the primary source of net rotor hub loads at low frequencies is the integrated aerodynamic loading developed on the blade.

Rotor motion measurements on earlier rotor systems made extensive use of discrete hinge locations for installation of rotary-motion transducers. These were often low-noise potentiometers, although more recent instrumentation systems have used RVDT devices. Measurements of blade flapping motions on hingeless rotors (such as the BO-105, Ref. 17) have used strain gauge measurements at locations pre-calculated to be "effective flapping hinges", based upon the blade spanwise flexibility and mass distribution. Calibration is performed through either static loading or limited thrust ground run-up tests. Thus, rotor blade motion measurements were always aircraft-specific and customized to the particular testing program data requirements.

The work conducted here for a Phase-I investigation is a result of previous efforts by the Principal Investigator and associates to apply active control technology to improve the performance, reliability and handling qualities of rotorcraft through direct feedback of rotor states to the flight control system. Estimation of rotor states has been attempted in the past both in system identification applications as well as for automatic controllers for aircraft and wind tunnel models. Virtually all of the schemes used involved recursive, sequential estimators to extract the state variables of interest. The various approaches may be subdivided into those that are "model-based", which include some form of predictive element in the estimator that mimics the rotor differential equations, or non-model-based, which resort to using either simplified approximations or particular sensor arrangements for this predictive information. Since the output of a rotor state estimator will most likely be used with a control law designed assuming full state feedback, careful choice of the state observer/estimator structure is important to providing a robust flight control system.

One of the first attempts to use modern state estimation schemes for rotor dynamics was by Briczinski and Cooper (Ref. 18), in which rotor blade flapping measurements were combined to estimate rotor coning and tip-path-plane (TPP) tilt degrees of freedom. Since the measurements were made in the rotating frame, time-varying transformations were necessary to process the flap angle transducers. In addition, the system dynamics for rotor flapping response were approximated using a random walk (Brownian motion) model in the estimator dynamics. DuVal (Ref. 19), in a simulation study, investigated designing TPP estimators by designing state observers around previously transformed blade flapping data. He also included estimation of TPP rate using both transformed flap and flap rate data, while similarly modeling blade dynamics as a random walk process. The resulting observer structure eliminated the need to propagate state covariance estimates in time.

Fuller (Ref. 20), in a different simulation study, investigated TPP estimation using data from a single blade as a means of accommodating possible failures using weighted multiblade measurements. Blade flapping acceleration was modeled as a first-order correlated process with time constant of one-quarter rotor period.

While these efforts concentrated on the use of angle transducers mounted directly on the rotor hub hinge points, such an approach would not be practical on non-articulated helicopter hubs or those with elastomeric bearings, due to the lack of a well-defined hinge point for such instrumentation. Efforts to address this deficiency have been made by researchers at the Royal Aircraft Establishment (RAE) (Ref. 21), where strain gauge data has been used in a regression technique to extract rotor modal motion from flight test data. The method, called "strain pattern analysis" (SPA), involves the calibration of a non-rotating instrumented blade under various loading conditions in terms of its measured deflections and resulting strain gauge signals. The associated patterns of gauge voltages are then used to reconstruct the modal participation of the rotor blade motion during actual flight operation. This technique has evolved to a promising state of development, but suffers from the fact that in-flight (rotating) blade mode shapes have significantly different second derivatives than those for non-rotating blades. As a consequence, the SPA "basis functions", determined through ground testing, are often not a sufficiently suitable set of patterns to capture the resultant blade motion in flight. In addition, this methodology requires the installation of a large number of strain gauges on a rotor blade, with all their attendant wiring and signal conditioning.

Modern articulated rotor systems present a design challenge for measurement of rotor deflections, due to an increasing trend to incorporate elastomeric bearings in the hub attachments. The UH-60A and SH-60 have used a blade root linkage, called a "crab arm", for determination of rigid body blade position through rotation sensors at three of its joints (Refs. 22, 23). Recombination of these sensor signals to compute blade flap, lag and pitch motion involves complex nonlinear transformations, and requires a complicated post-installation calibration procedure to assure proper measurement accuracy.

Rotor structural loads estimation has traditionally been performed using strain gauge sensors mounted on the rotor shaft and/or pitch link assemblies (e.g., Ref. 24), although one of the blades of the UH-60A of Ref. 23 had a series of over 30 strain gauges mounted on its surface. A different technique that avoids rotating-frame instrumentation (for production aircraft), developed by Kaman Aircraft, uses a transfer-function representation of the coupled helicopter-rotor system to estimate rotor loads from fuselage mounted instrumentation (Ref. 25, 26). This method, called "force determination", or "holometrics", requires a calibration of the fuselage sensors through a regression analysis that uses rotor measurements from an instrumented flight test or ground shake test. A linear relationship is assumed between the two systems, and thus the fuselage sensors may infer what the rotor system loads are through application of this identified transfer function. This method has the obvious drawback of requiring a complete flight test of a target aircraft to determine these transfer function relationships in order to extract rotor loads information from a production vehicle using fixed-frame-only instrumentation. Such a limitation would invalidate its use in a flight test environment, but makes it suitable for fatigue life monitoring on fleet aircraft.

The innovation investigated under this Phase-I effort for measurement of rotor motion and loads is a byproduct of research aimed at providing rotor state estimates for use in Individual Blade Control (IBC) applications (Refs. 13-14, 27-35). By incorporating acceleration measurements directly into the state observer, this method does not require a complex predictive element in the estimator structure, leading to an extremely simple, time invariant filter. Rotor state estimation thus can be performed directly on the rotor blade, if

desired, eliminating the requirement to transfer many signals from the rotating to the nonrotating system. Use of accelerometers, while more expensive than strain gauge sensors, provides a more flexible and robust means of estimating rotor motion with minimal impact upon rotor hub installation requirements. This fact was amply demonstrated in References 30 and 31, where simple clamp-on devices were used to sense both flap and lag motion of a NASA full-size wind tunnel rotor system.

Research related to that conducted here for this Phase-I study, albeit on a reduced scale, was recently undertaken by the Principal Investigator while at Princeton University (Ref. 33). This work addressed the practical issues associated with measuring rotor blade elastic out-of-plane motion using spanwise-mounted accelerometers, and developed an on-blade serial digital data acquisition system for measuring up to 11 differential analog transducer channels. This system was modeled after work by NASA (Ref. 36), in which a digital data acquisition system was mounted on the rotor blade for measuring blade bending loads and pressures. The data for this latter system was telemetered to both the test aircraft fuselage and to ground recording stations.

Finally, the helicopter community is not alone in their requirements for extracting data from a rotating blade to determine blade loads and vibratory motion. The wind turbine industry, concerned with the fatigue life and continued operational usage of their rotor systems, has invested considerable time and energy into developing data collection system for monitoring wind turbine rotor performance and loads. As described in Ref. 37, these systems include capabilities for remote data collection over conventional phone lines (since the rotors are often located at remote rural sites), and often use slip rings for transferring data and power from the rotating system to the support towers, although more advanced units have employed low power telemetry for pulse code modulated (PCM) signal transmission (Ref. 38).

1.3 Outline of Current Approach

In order to gain an appreciation for the advantages inherent in the use of Kinematic Observers for rotor modal displacement and loads measurement, a simple example will be developed that contrasts the proposed technique with a more conventional model-based estimation scheme.

Modern estimation theory (Ref. 39, 40) provides a formalism for the extraction of information from data that may come from a wide variety of sensors. The mathematical basis for estimation theory makes extensive use of linear algebra to conveniently describe the sensor output, noise sources, and the variables being estimated in terms of vector quantities. This representation allows incorporation of the system dynamics and sensor measurements into a compact notation, and thus reformulates the description of a dynamic processes in terms of a set of first-order vector equations involving "state variables". For this particular application of this Phase-I proposal, these "states" would represent physical motion of the rotor dynamic modes, such as blade flapping position, flap rate (velocity), lag position, lagging rate, and so on.

Given a possibly nonlinear and time-varying set of first-order differential equations of the form:

$$\dot{\mathbf{x}}(t) = \mathbf{f} \{ \mathbf{x}(t), \mathbf{u}(t), t \} \quad (1.1)$$

where $\mathbf{x}(t)$ represents an N-dimensional state vector of rotor displacements and velocities, $\dot{\mathbf{x}}(t)$ represents its associated time derivative, $\mathbf{u}(t)$ is an M-dimensional forcing function (e.g., of control, wake and gust inputs), and \mathbf{f} is the possibly nonlinear and time-varying function relating the two vector quantities to the time rate of change of the state vector, we wish to estimate the trajectory, or time history, of $\mathbf{x}(t)$ using noise-corrupted measurements:

$$\mathbf{y}(t) = \mathbf{h} \{ \mathbf{x}(t), \mathbf{u}(t), t \} + \mathbf{n}(t) \quad (1.2)$$

with $\mathbf{y}(t)$ representing the L-dimensional vector of sensor measurements, $\mathbf{n}(t)$ an L-dimensional vector of additive noise, and \mathbf{h} the possibly nonlinear and time-varying algebraic relationship between the system states, inputs and measurements. Estimation theory maintains that under certain cases, the estimation errors of the states can be exponentially driven to zero by coupling a model of the system dynamics with a feedback term proportional to the residual between the predicted output and the actual system measurement. For this to be true, the system must be "observable", which requires that certain conditions relating the dynamics of the process and the types of measurements available must be met. These requirements ensure that the measurements are influenced by all the state variables, and that measured combinations of the states are separable due to differing dynamic processes.

The state estimator has the general form:

$$\dot{\hat{\mathbf{x}}}(t) = \mathbf{f} \{ \hat{\mathbf{x}}(t), \mathbf{u}(t), t \} + \mathbf{K}(t) [\mathbf{y}(t) - \mathbf{h} \{ \hat{\mathbf{x}}(t), \mathbf{u}(t), t \}] \quad (1.3)$$

where the first term constitutes a prediction of the time rate of change of the state vector, and the second term a correction proportional to the detected differences between the sensor measurements and their predicted values, based upon the current state variable estimates. This difference between the sensor outputs and their predicted values, called the measurement residual, provides the "feedback" term in the state estimator and is responsible for reducing the vector of estimation errors ($\hat{\mathbf{x}}(t) - \mathbf{x}(t)$) to zero. This predictor - corrector scheme is common to all observers, and differs only through the choice of the prediction model and the computation of the correction term proportionality factor (or, gain matrix) $\mathbf{K}(t)$ (Ref. 40). For a standard Kalman Filter implementation, the gain $\mathbf{K}(t)$ is determined by minimizing the estimation error covariance based on assumed noise statistics for the forcing function $\mathbf{u}(t)$ and the measurement noise $\mathbf{n}(t)$.

Special consideration must be given when accelerometers are used as part of the sensors available for measurement. Since most system's dynamics equations involve application of Newton's second law, it is often unnecessary to include accelerations as state variables in the representation of a body's dynamic equations of motion. Acceleration quantities are typically just the time derivatives of the velocity states, and thus the representation of an acceleration measurement is made by incorporating the system's dynamic equations of motion. That is, if the "i-th" measurement is of the "j-th" state variable's acceleration, where the "j-th" state represents a particular displacement, and the "j+1-th" state represents its associated velocity, then:

$$\mathbf{y}_i(t) = \ddot{\mathbf{x}}_j(t) = \dot{\mathbf{x}}_{j+1}(t), \text{ where } \mathbf{x}_{j+1}(t) = \dot{\mathbf{x}}_j(t) \quad (1.4)$$

and thus from the "j+1-th" differential state equation,

$$\dot{\mathbf{x}}_{j+1}(t) = \mathbf{f}_{j+1} \{ \mathbf{x}(t), \mathbf{u}(t), t \} \quad (1.5)$$

so that the "i-th" measurement equation is now the possibly nonlinear and time-varying "j+1-th" dynamics equation, or,

$$\mathbf{y}_i(t) = \mathbf{h}_i \{ \mathbf{x}(t), \mathbf{u}(t), t \} = \mathbf{f}_{j+1} \{ \mathbf{x}(t), \mathbf{u}(t), t \} \quad (1.6)$$

The primary difficulty with the above approach is that the predictive component of the estimator is dependent upon the assumed model structure of the dynamic system whose states are being estimated, or "observed". In addition, the use of accelerometer measurements in this manner complicates this problem by introducing some of the same dynamic model equations into the representation for the sensor output. This situation can become particularly troublesome if an accurate model of the system dynamics is not readily available, is very complex, or has unmeasurable inputs. For most helicopter rotor systems, all three of these limitations often apply, due to the complex aeromechanical interactions encountered in flight. As the dynamic system model becomes more complex, so also do the computational requirements of the state estimator, and similarly, its sensitivity to potential modeling errors. What is needed is an improved procedure for estimating rotor state variables (i.e., rotor blade position and velocities).

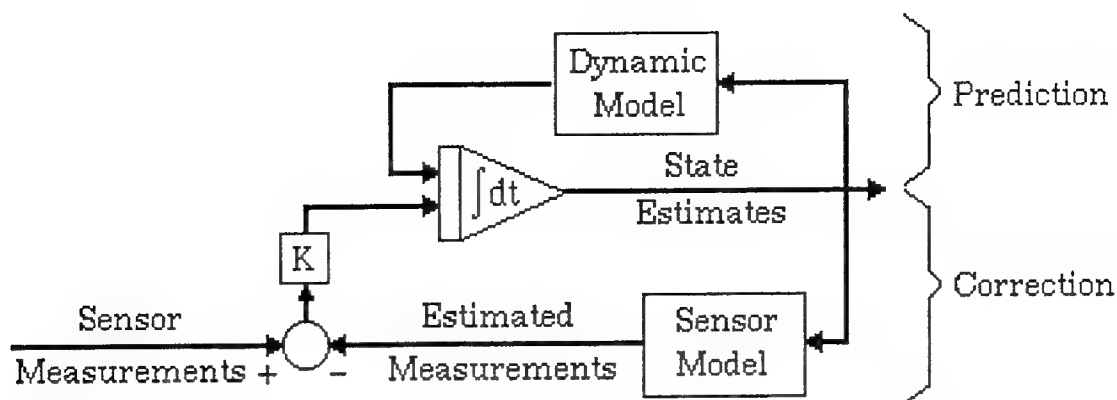
Fortunately, such an improved methodology exists. Kinematic Observers avoid the above problem identified above by using the acceleration measurement directly as predictive information, bypassing the need to incorporate mathematical dynamics models into the expressions for sensor content (Refs. 27-34). That is, one rewrites the above state estimator equation to appear as:

$$\dot{\hat{\mathbf{x}}}_j(t) = \hat{\mathbf{x}}_{j+1}(t) + \mathbf{K}_j(t) [\mathbf{y}_{i-1}(t) - \hat{\mathbf{x}}_j(t)] \quad (1.7)$$

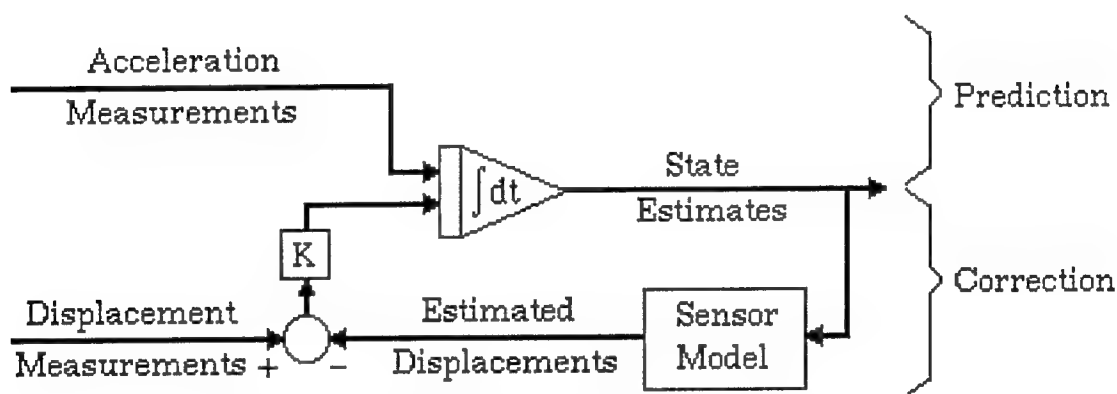
$$\dot{\hat{\mathbf{x}}}_{j+1}(t) = \mathbf{y}_i(t) + \mathbf{K}_{j+1}(t) [\mathbf{y}_{i-1}(t) - \hat{\mathbf{x}}_j(t)] \quad (1.8)$$

where $\mathbf{x}_j(t)$, $\mathbf{x}_{j+1}(t)$, and $\dot{\mathbf{x}}_{j+1}(t)$ represent a rotor blade position state variable, velocity state variable, and acceleration, respectively, and $\mathbf{y}_{i-1}(t)$ and $\mathbf{y}_i(t)$ are a position and acceleration measurement. As is readily apparent, no representation of the system dynamics is required, since one achieves the prediction portion of the observer by direct use of the acceleration measurement. The corrective action is supplied through feedback of the position measurement residual, with the estimation errors driven to zero at a rate proportional to the magnitude of $\mathbf{K}(t)$.

Kinematic Observers can thus be viewed as an alternative to traditional model-based state estimation approaches, for the case when sufficient sensor information exists to reconstruct modal acceleration data. That is, there must be a sufficient number of accelerometer sensors to uniquely determine all the accelerations of the various rotor modes to be estimated using this approach. In its simplest form, a Kinematic Observer replaces the predictive capability of a system dynamic model with a direct acceleration measurement. Figure 1.1 graphically illustrates the approach described here by comparing a block diagram representation of a traditional state estimator with that of a Kinematic Observer.



Conventional State Estimation Approach



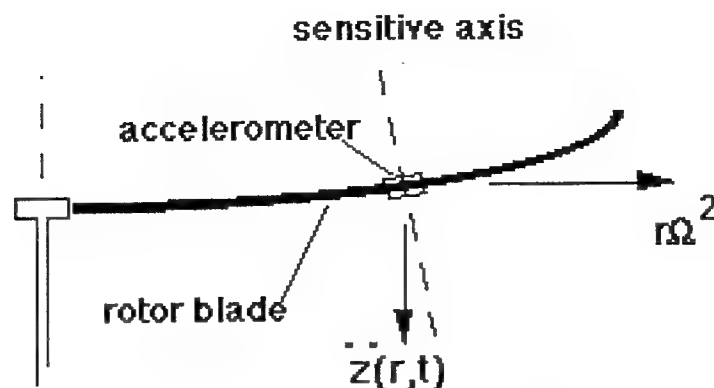
Kinematic Observer State Estimation Approach

Figure 1.1: Block diagram comparison of conventional and Kinematic Observer rotor state estimators

The use of accelerometer sensors for rotor motion measurement has additional benefits. Since rotor blades operate in a very strong centrifugal field, blade-mounted accelerometers will sense any blade displacements that cause their sensitive axis to have a component parallel to this centrifugal acceleration. Figure 1.2 shows the signal content of an accelerometer whose sensitive axis is oriented perpendicular to the surface of the blade, so as to measure blade motion out of the plane of rotation. Two accelerometers mounted in different spanwise locations would provide enough information to determine rigid blade flap displacement and flapping acceleration (via solving two equations in two unknowns). By locating these accelerometers both spanwise and chordwise on the rotor blade, it becomes possible to sense blade flap, lag, torsion, and various bending motions without the use of any blade root instrumentation. This result implies that a rotor system measurement scheme that uses accelerometer sensors is not required a priori to accommodate a particular hub geometry and hence would have a wide applicability to a number of different helicopter types.

To further illustrate this point, if several accelerometers were located along the span of a single blade, then Fig. 1.2 shows that by representing the out-of-plane displacement in terms of a modal expansion, each accelerometer would sense a component of modal acceleration proportional to its modal displacement at that spanwise location, and a

component of modal displacement, proportional to the sensor spanwise location multiplied by the local mode shape slope at that point. Thus, every added accelerometer contributes an additional measurement of modal acceleration and modal displacement for all modes considered.



$$\begin{aligned}
 accel(r,t) &= \ddot{z}(r,t) + r\Omega^2 \frac{\partial z(r,t)}{\partial r} \\
 \text{for } z(r,t) &= \sum_i \eta_i(r) q_i(t), \\
 accel(r,t) &= \sum_i \left\{ \eta_i(r) \ddot{q}_i(t) + r\Omega^2 \frac{\partial \eta_i(r)}{\partial r} q_i(t) \right\}
 \end{aligned}$$

Figure 1.2: Accelerometer signal content for flapwise mounted sensor.

Three primary observations can thus be made: (1) use of accelerometer sensors, in sufficient numbers, allows sensing of blade structural modal response, in addition to merely providing rigid blade motion information; (2) proper representation of the signal content of each accelerometer sensor depends upon a good description of the natural modes of the rotor blade; and (3) although N modal accelerations and displacements may be determined uniquely using N distributed accelerometer sensors, the possibility exists for additional robustness through additional $(N+P)$ sensors to be combined in a "least squares" estimate of N modal accelerations and displacements. Each of these topics is further discussed in subsequent sections of this report.

Finally, an additional application may be made of this accelerometer data to determine flight loads. Since the Kinematic Observer methodology can determine modal accelerations, modal velocities and modal positions, system identification techniques may be used to estimate the parameters of the dynamic process that govern their interrelationship. Such an approach is equivalent to an "equation-error" estimation of the system dynamics, in that the identification technique determines the best-fit equation coefficients that are consistent with the given estimated state values for a prescribed dynamic model structure (Refs. 40, 41). These equation coefficients would include the modal "mass", "spring", and "damping" terms along with the modal forcing function. Reference 28, for example, used this technique to determine the parameters of the flapping response equation from model rotor data. While such a technique is mathematically possible, in actual implementation it is anticipated that a fairly large number of rotor blade modes would be required to capture the spanwise variation of aerodynamic forcing, and thus, this technique may be of only limited utility.

A variant on this approach, however, shows promise for providing loading information if the rotor blade structural properties are used to identify both blade shear and moment "modes", as is typically done using a Holzer-Myklestad analysis (Ref. 42). Such an approach allows for treating the rotor blade as an "equivalent load cell", and thus one may infer what loads have been applied to it by measuring its structural response. More details of this technique are presented in the section on load reconstruction.

1.4 Phase-I Research Tasks and Final Report Outline

The work performed for this Phase-I study identified the technological challenges apparent in the proposed instrumentation scheme, and addressed their impact on the capability of the system to extract rotor motion and loads data during flight operations. The assessment was conducted through analysis using simulated rotor responses, and via experimental demonstration on an instrumented Froude-scaled model rotor system. A large portion of the analytical work involved the use of simulation and borrowed concepts from an inverse model of the rotor response (Ref. 43), in order to address potential problem areas in the implementation of the accelerometer-based instrumentation scheme. The simulation code used is described in Section 2, and the results of the analytical work are presented in Section 3. These included addressing potential sources of measurement error associated with the sensor measurement equations, the effect of using a truncated natural mode series for representing rotor motion degrees of freedom, the problems inherent in the use of poorly chosen mode shapes for representing rotor motion, the effect of sensor biases and other sensor-related errors, the selection of optimal locations for sensor placement, and the capability to reconstruct rotor loads through measurement of distributed blade accelerations.

A description of the model rotor test hardware, used in demonstration testing of the approach for flapping position estimation, is given in Section 4, along with the results from the hover tests of an instrumented blade. Implementation issues associated with the development of the concept to flight hardware are addressed in Section 5. Finally, conclusions from the Phase-I work are presented in Section 6, a work plan for a proposed Phase-I Option effort is proposed in Section 7, and then some recommendations for a complete investigation into taking this instrumentation concept toward prototype development are given in Section 8. A complete list of references cited in the report appears in Section 9.

2.0 SIMULATION DEVELOPMENT

Two simulations were used in the analysis effort under this Phase-I project. The first was a simplified time-marching representation of a single rotor blade, for use in investigations concerning the transient characteristics of the instrumentation scheme in reconstructing rotor modal response. Portions of the code for this simulation were new developments as part of this SBIR effort, and thus part of the validation of the extensions to this analysis included comparisons with the second simulation tool used, CDI's RotorCRAFT code. A description of the features associated with the single blade forced response simulation are given below, whereas the RotorCRAFT code is described in detail in Ref. 44.

2.1 Transient Rotor Blade Simulation Features

2.1.1 General

An analytical model for single rotor blade motion and loads sensing sensitivity studies was developed during this Phase-I work. This model represents a single-blade time-stepping analysis, with capability for a variety of sensor output models, and sufficient flexibility for including a complete modal description of flap, lag, and torsional displacements. These motions can be the result of both discrete hub hinge geometry degrees of freedom and elastic deflections of the blade structure. Representation of the rotor degrees of freedom is provided as an input file from the user, along with information on the operating state of the rotor (or, flight condition of the helicopter), and initial conditions for the rotor modal displacements.

A time-marching approach was selected over a frequency-domain model (as is typified by harmonic balance approaches), since this would provide the needed flexibility of the analytical model to properly represent transient behavior of the rotor motion and loads sensing scheme. This formulation also allows for easy incorporation of any control or estimation systems modeling, as these are often formulated in the time domain as well. Thus, the simulation may also be extendible to incorporate a variety of detailed transient signal modeling of the distributed sensor suite proposed for the measurement system under this proposal.

2.1.2 Structural Model

Although the mathematical model has been developed using linearized modal-based equations of motion (e.g., Ref. 45), additional subroutines have been added to allow for proper representation of nonlinear effects as well. These may include particular geometric nonlinearities due to elastic deflections in a centrifugal force field, and the like (Ref. 46). Blade modal properties may be pre-computed using a companion program that reads in the blade's distributed structural properties and computes mode shapes, or they may be supplied directly in terms of either polynomial shape functions or coefficients of transcendental functions. Explicit functional forms for the mode shapes are required in order to accurately compute blade slopes at sensor locations, and thus, properly represent the signal content of distributed sensors such as accelerometers and strain gauges.

2.1.3 Aerodynamic Model

Aerodynamic loads are computed in a separate subroutine, that through a combination of common arrays and calling parameters provides sufficient flexibility to

allow use of a wide range of aerodynamic models. These models have ranged from simple inflow representations for computing local blade section angle of attack, to coupling with the rotor inflow computed from the C.D.I. RotorCRAFT helicopter curved-vortex element performance analysis. In this fashion, varying levels of detail may be added to the aerodynamic model in order to either improve fidelity of the simulation (at the cost of code turnaround time), or to study the sensitivity of the results to the aerodynamic model used. The flexibility in the model will allow for future extensions to handle high-inflow simulations, such as would be represented by high climb rates or highly-twisted rotor configurations like those on the V-22 Osprey.

2.1.4 Hub Loads Calculation

The code computes hub loads (for a single blade) using a force-summation approach (Ref. 42), since the time-integration formulation allows for easy determination of inertial loads. This latter requirement was imposed by the need to properly represent distributed accelerometer signals as part of the proposed rotor motion and loads measurement scheme.

2.1.5 Verification and Validation

Verification and validation of the simulation code was performed through simple comparisons with analytical models (Ref. 47), more sophisticated analyses (Ref. 44), and test data (Ref. 48). This exercise assured that the results from the simulation exercises may be used with confidence in the design of experiments on both model and full-scale rotor systems in the future.

2.2 Simulation Goals Under Phase-I

Goals of the simulation studies were directed toward: (a) assessing the accuracy of the proposed measurement technique in both reconstructing rotor motion and loads information; (b) determining the required type and accuracy of pre-test information on the test aircraft, and on the instrumentation's location on the rotor system, in order to provide acceptable measurements of rotor blade position and loads; (c) investigating the tradeoffs present between transient response of the measurement system and the potential for generating excessive "noise" from unmodeled high-frequency modal response entering the sensor outputs; (d) providing design guidance on the impacts of sensor errors and how to avoid or mitigate them; and (e) studying various schemes for providing self-test and/or self-calibration features with this instrumentation system.

While these studies did not investigate every avenue associated with each of these potential problem areas for the measurement scheme, sufficient evidence of anticipated performance was generated to provide for evaluation of the suitability of the accelerometer-based technique in measuring rotor motion and loads. The results from each of these investigations are presented in the next section.

3.0 SIMULATION RESULTS

3.1 Accuracy Assessment

One of the key questions asked of any instrumentation system proposed for taking measurements is the overall expected accuracy of the system. If the resultant accuracy is not sufficient for the purpose of the flight test program, the instrumentation is worthless. Accuracy may be readily specified for discrete sensors, such as potentiometers mounted on hinge joints, but for systems that employ dynamic signal processing as part of the measurement production, the accuracy must be computed using estimation theory (Ref. 39). In order to appreciate how errors may propagate through the estimation process, however, one must first consider the form of the dynamic signal processing used (i.e., the Kinematic Observer) and the method of generating modal acceleration and displacement information. Development of both the Kinematic Observer equations, and a fundamental assessment of potential sources of accuracy, is provided below using an example directed at a rigid blade flap estimation application.

3.1.1 Instrumentation Requirements of the Methodology

Two fundamental features are present in the sensing technique described here. The first of these, which is essential to the development of the Kinematic Observer, is the use of accelerometer signals as a predictive indication of the blade's response. Use of accelerometers provides a signal that may be integrated forward in time (with appropriate compensation of bias errors) to provide an estimate of the blade modal velocity and position. The second required feature is the use of these accelerometers in a rotating (hence, accelerating) reference frame, so that displacements within that reference frame may generate significant accelerations that are detectable by the accelerometers. Without a suitable position reference, there would be no means of compensating for bias offsets on the accelerometer in the integration process. Thus, if an alternate means of sensing position is available, this could be used as a "replacement" sensor for one of the accelerometers to be used. As will be seen in the discussion later, this fact becomes important for sensing rotor flapping motion on a teetering rotor using this technique.

The net result is that the technique requires a minimum instrumentation list according to the number of degrees of freedom required for measurement. For each mode to be sensed, one requires a measurement of the modal acceleration, and a measurement of the modal position. These measurements may not be directly available as the pure output from a sensor, but should be reconstructable from available sensor data. In the previous applications of this method cited in the References, this was often accomplished through a matrix inversion operation, or equivalently, the solution of n linear equations for n unknowns. Hereafter in the discussion, these reconstituted signals will be referred to as the "measurements" of modal acceleration and position. The methodology then takes the acceleration measurement, integrates it forward in time twice, and generates a position estimate. That position estimate is compared to the position measurement for that mode, and the error is fed back (with appropriate gain) to both integration passes in order to drive the estimation error exponentially to zero.

This ideal state of having the estimation error approach zero will occur when all the conditions of a standard recursive linear filter apply: the "system" must be observable (which it is, if we do indeed have both position and acceleration measurements), and the measurements of the acceleration and position of the mode must be unbiased. This latter requirement typically means that one must guard against bias on the accelerometer through

one of several possible techniques. The first of these is to select accelerometers that have exceptional DC drift specifications, and hence assume that the accelerometers are unbiased. This is the approach taken by the instrumentation engineers at NASA Ames on the UH-60 RASCAL aircraft (Ref. 50). A second approach for bias accommodation is to include an additional "state" to be estimated, which represents this bias state, in the observer formulation. This then requires an "absolute" position reference that is unbiased, as would be available from a non-accelerator transducer, such as a potentiometer. This approach has been taken in the post-processing of some model rotor data for IBC tests conducted at M.I.T. Note that this approach would not work for an "accelerometer only" sensor suite, since there would be no absolute reference from which to estimate the bias signals. Put in mathematical terms, an accelerometer-only measurement scheme that included bias states with each accelerometer would not constitute an "observable" system. A third method would be to provide for some form of auto-zeroing of the accelerometer output during initial power-up, in order to accommodate any bias that may have crept into the sensor over time. Finally, the last method is to forgo the attempt to measure static response, and filter all signals with a high-pass network (or "AC-couple" them) at some sufficiently low frequency. For the helicopter case, this approach would make it possible to then estimate, for example, first-harmonic flapping (and higher frequency modal responses), while not allowing reconstruction of steady rotor coning angle.

Use of accelerometer sensors to "drive" the estimation approach allows the replacement of the typical predictive structure in an estimator with the acceleration signal directly. This means that one does not have to rely on a detailed mathematical model of how the system changes in time (i.e., the describing differential equation) in order to predict the modal position in the future; it can be found directly through integration, a "data smoothing" operation. This is the primary attraction of the methodology for helicopter rotor applications, in that complicated models of the rotor blade motion are not required to obtain smooth estimates of its response. The difference, then, between conventional estimation techniques and the current method is one of mathematical models: conventional approaches require both a model of the process and the sensors; the current approach only requires an understanding of the *kinematics* of the process and a model of the sensors (hence the name Kinematic Observer). For a helicopter rotor, this is a sizable difference. A comparison of the block diagrams of each of these approaches was shown previously in Figure 1.1.

3.1.2 Demonstration on a Spring-Mass-Damper System

In order to more fully appreciate the fundamental differences in these two estimation approaches, some basic estimation studies may be performed on a simple one-dimensional system. As shown in Figure 3.1 below, this system is merely a sprung mass with a damper, with an accelerometer located on the mass. A second transducer is also presumed to be available to measure the relative motion of the mass above the mounting point.

The equation for this system may be found in any sophomore text on dynamics as:

$$m\ddot{x}(t) + c\dot{x}(t) + kx(t) = f(t) \quad (3.1)$$

where m is the sprung mass, c is the damper constant, k is the spring constant, $f(t)$ is the applied force on the mass, $x(t)$ is the displacement, and dots indicate time derivatives of quantities.

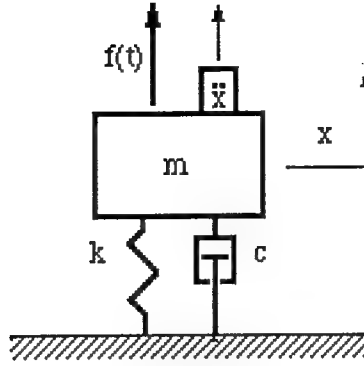


Figure 3.1: Sprung mass example problem for Kinematic Observer formulation.

Sensor measurements of this system consist of acceleration $\ddot{x}(t)$ and position $x(t)$. The sensor and mathematical model may be combined into state-space form as:

$$\begin{aligned} \begin{Bmatrix} \dot{x}(t) \\ \ddot{x}(t) \end{Bmatrix} &= \begin{bmatrix} 0 & 1 \\ -k/m & -c/m \end{bmatrix} \begin{Bmatrix} x(t) \\ \dot{x}(t) \end{Bmatrix} + \begin{Bmatrix} 0 \\ f(t)/m \end{Bmatrix} \\ \begin{Bmatrix} y_1(t) \\ y_2(t) \end{Bmatrix} &= \begin{Bmatrix} x(t) \\ \ddot{x}(t) \end{Bmatrix} = \begin{bmatrix} 1 & 0 \\ -k/m & -c/m \end{bmatrix} \begin{Bmatrix} x(t) \\ \dot{x}(t) \end{Bmatrix} + \begin{Bmatrix} 0 \\ f(t)/m \end{Bmatrix} \end{aligned} \quad (3.2)$$

Note in particular that since we are using an accelerometer as a sensor, the dynamics of the system appear in the sensor equations as well. While this is not an issue for this simple problem, in the case of helicopter rotor dynamics, these equations would be periodically time varying in forward flight, as well as having nonlinear dependence upon the rotor wake structure.

A Kinematic Observer formulation of this same problem treats the acceleration as a random process, and thus simplifies the dynamics according to:

$$\begin{aligned} \begin{Bmatrix} \dot{x}(t) \\ \ddot{x}(t) \end{Bmatrix} &= \begin{bmatrix} 0 & 1 \\ 0 & 0 \end{bmatrix} \begin{Bmatrix} x(t) \\ \dot{x}(t) \end{Bmatrix} + \begin{Bmatrix} 0 \\ a(t) \end{Bmatrix} \\ \begin{Bmatrix} y_1(t) \\ y_2(t) \end{Bmatrix} &= \begin{Bmatrix} x(t) \\ \ddot{x}(t) \end{Bmatrix} = \begin{bmatrix} 1 & 0 \\ 0 & 0 \end{bmatrix} \begin{Bmatrix} x(t) \\ \dot{x}(t) \end{Bmatrix} + \begin{Bmatrix} 0 \\ a(t) \end{Bmatrix} \end{aligned} \quad (3.3)$$

Now the acceleration $a(t)$ is treated as an *input* to the system that is measurable, and thus the dynamic representation simply states that modal velocities are time derivatives of modal positions, etc. The representation of the system is now just two time integration operations, with measurements of the input to the first and of the output from the last. This formulation is extremely simple and has constant coefficients for all system representations (including rotor dynamics), and thus a "state estimator" designed for estimating position and velocity would be very simple, as will be shown below.

State estimators for linear systems are of the form:

$$\begin{aligned} \dot{\hat{x}} &= A\hat{x} + Bu + K(y - \hat{y}) \\ \hat{y} &= C\hat{x} + Du \end{aligned} \quad (3.4)$$

where x , y and u are vectors of the states, outputs and control inputs, respectively, of the dynamic system; A and B are the system dynamics and control effectiveness matrices; and C and D are matrices describing the sensor outputs in terms of both the states and the control inputs. Hatted quantities in the above equation indicate estimated values, while K is a feedback gain matrix that will eventually drive the state estimates to track the actual states, if picked correctly.

Since we are considering two different forms for representing the system dynamics for the sprung-mass example, we will have two approaches for estimating the states of the system, namely, the position and velocity of the mass. For the system of equation (3.2), this becomes:

$$\begin{Bmatrix} \dot{\hat{x}}(t) \\ \ddot{\hat{x}}(t) \end{Bmatrix} = \begin{bmatrix} -K_{11} + K_{12}\left(\frac{\hat{k}}{m}\right) & 1 - K_{12}\left(\frac{\hat{c}}{m}\right) \\ -\left(\frac{\hat{k}}{m}\right) - K_{21} + K_{22}\left(\frac{\hat{k}}{m}\right) & -\left(\frac{\hat{c}}{m}\right) + K_{22}\left(\frac{\hat{c}}{m}\right) \end{bmatrix} \begin{Bmatrix} \hat{x}(t) \\ \dot{\hat{x}}(t) \end{Bmatrix} + \begin{bmatrix} K_{11} & K_{12} \\ K_{21} & K_{22} \end{bmatrix} \begin{Bmatrix} y_1(t) \\ y_2(t) \end{Bmatrix} \quad (3.5)$$

and for the system of equation (3.3), the form is:

$$\begin{Bmatrix} \dot{\hat{x}}(t) \\ \ddot{\hat{x}}(t) \end{Bmatrix} = \begin{bmatrix} -K_{11} & 1 \\ -K_{21} & 0 \end{bmatrix} \begin{Bmatrix} \hat{x}(t) \\ \dot{\hat{x}}(t) \end{Bmatrix} + \begin{bmatrix} K_{11} & 0 \\ K_{21} & 1 \end{bmatrix} \begin{Bmatrix} y_1(t) \\ y_2(t) \end{Bmatrix} \quad (3.6)$$

where "hatted" quantities have been used to represent estimates of either states or system properties.

Several observations may be made from the comparison of these two forms of state estimator. The first and most important is that the general form shown in equation (3.5) has an explicit dependence upon the estimated values of the system parameters, and thus, may be sensitive to modeling errors present in the representation of the system. While these would be small for the simple single degree-of-freedom sprung mass illustrated here, they could be significant for nonlinear, periodic systems such as helicopter rotors. Second, whereas the "input" for the system ($f(t)/m$) represented by equation (3.2) is not "measured" explicitly and hence shows up only implicitly in the estimator in (3.5), it is treated like an input in the estimation approach of equation (3.6), due to the selection of the gains $K_{12} = 0$ and $K_{22} = 1$. Finally, while the format of (3.5) allows for many choices of the gain matrix K to achieve a particular set of state estimator pole locations, this freedom is not present in (3.6) due to the restriction of only two free parameters. This limitation is trivial, however, because the two gains allow arbitrary placement of the two observer poles, and thus the apparent additional design freedom is not of any significance.

3.1.3 Application to Flapping Motion Estimation

Application of Kinematic Observers for measurement of rotor blade flapping using spanwise mounted accelerometers is now developed, and as will be seen below, is dependent upon the particulars of the hub geometry. To appreciate this dependence, a general hub arrangement of an offset-hinge-plus-hub-spring model of the rotor hub will be used, from which specific rotor types could be approximated through limiting values on the offset distance or spring value.

The dynamic equation of motion that describes rotor blade out-of-plane motion (flapping motion) for an offset-hinged articulated rotor with hub spring may be written as:

$$\beta^{**}(\psi) + v_{\beta}^2 \beta(\psi) = f(\theta, \lambda, \mu, \gamma, \beta, \beta^*, \psi) \quad (3.7)$$

where

| | |
|---|--|
| $\beta(\psi)$ | represents the flap angle of the blade; |
| ψ | is the azimuth angle for the blade (nondimensional time); |
| $*$ | is a time derivative nondimensionalized by the rotor speed; |
| γ | is the Lock number, a ratio of aerodynamic forces to inertial forces on the blade; |
| λ | is an averaged rotor inflow velocity, nondimensionalized by rotor tip speed; |
| μ | is the advance ratio; |
| θ | is the average geometric pitch angle of the rotor blade; |
| v_{β} | is the nondimensional flapping frequency of the blade; and |
| $f(\theta, \lambda, \mu, \gamma, \beta, \beta^*, \psi)$ | is the integrated distributed aerodynamic moment about the flapping hinge. |

For the case of an accelerometer located spanwise some distance r from the hub, outboard of the flapping hinge (located at distance e), the accelerometer may be seen (from Figure 3.2) to contain components of both flapping acceleration and centrifugal acceleration according to:

$$accel(\psi)/R\Omega^2 = \frac{(r-e)}{R} \beta^{**}(\psi) + \frac{r}{R} \beta(\psi) \quad (3.8)$$

where

| | |
|----------|--|
| r | is the spanwise distance measured from the hub center; |
| e | is the distance of the flapping hinge to the hub center; |
| R | is the radius of the rotor; |
| Ω | is the rotor rotational speed. |

Note that the accelerometer signal has been nondimensionalized by the centrifugal acceleration at the rotor blade tip ($R\Omega^2$).

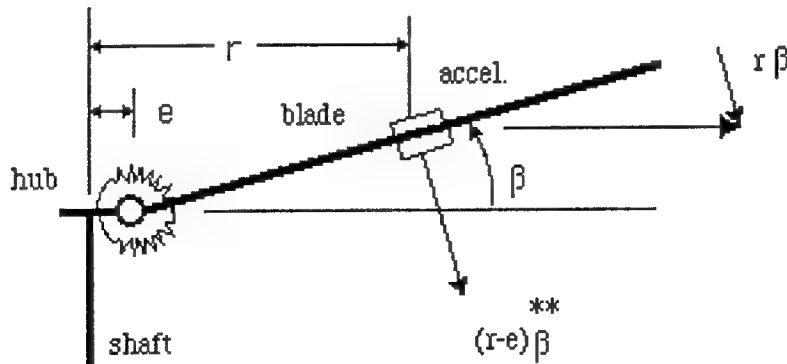


Figure 3.2: Accelerometer signal content schematic

The first term of equation (3.8) represents the inertial reaction of the blade flapping motion about the hinge, and the second is the component of centrifugal acceleration seen by

the sensor as the blade flaps up out of the plane of rotation. In more general terms, the first is approximately the vertical acceleration of the blade at that spanwise location, and the second is the centrifugal acceleration multiplied by the local slope of the blade at that spanwise station. Thus, for the case where all of the out-of-plane motion is represented only by rigid blade flapping, one arrives at the above expression of (3.8).

Notice now that this one accelerometer senses two of the desired unknowns: modal acceleration, *and* modal displacement. In order to unambiguously determine these two necessary "measurements" for use in the Kinematic Observer, an additional sensor is required for solving two equations for these two unknowns. This could be either a hub displacement (flap) sensor, mounted at the flapping hinge location, or an accelerometer, mounted at a *different* spanwise location. Since the one of the fundamental purposes of the proposed instrumentation schemes is to avoid the requirements for discrete hinge location measurements, we will consider the use of a second accelerometer sensor.

Representing the accelerometer locations for the above flapping sensor as r_1 and r_2 , the measurement equation may be written in matrix form as:

$$\begin{Bmatrix} a_1(\psi) \\ a_2(\psi) \end{Bmatrix} = \begin{bmatrix} \frac{r_1 - e}{R} & \frac{r_1}{R} \\ \frac{r_2 - e}{R} & \frac{r_2}{R} \end{bmatrix} \begin{Bmatrix} \beta^{**}(\psi) \\ \beta(\psi) \end{Bmatrix} \quad (3.9)$$

Provided that r_1 is distinct from r_2 , this matrix is invertible and one can solve uniquely for the flap position and acceleration. Since the r values must be bounded between e and R , one may investigate the "invertability" of this matrix, or, how close to singular this matrix is as a function of the sensor location. Singular matrices indicate that they are not of full rank (i.e., at least one row or column is a linear combination of other rows or columns), and the "condition number" of the matrix indicates the amplification factor that relative changes in the sensor signals (a_1 and a_2 here) can have on relative changes in the solution vector (flap acceleration and position in this case). Figure 3.3 below shows the variation of the inertial and the centrifugal term (first and second column elements, respectively) for the sensor content, as a function of spanwise sensor location, assuming a flapping hinge offset of 7% (i.e., $e/R = 0.07$).

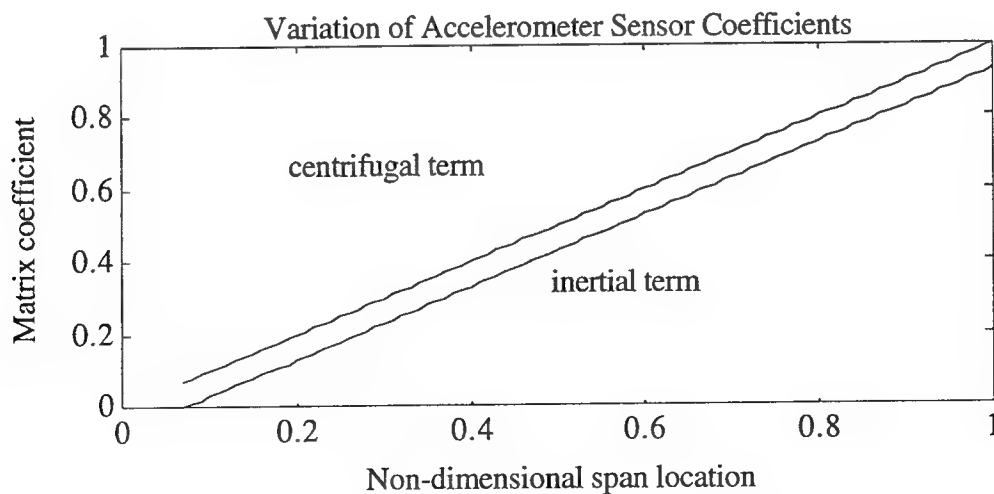


Figure 3.3: Variation of measurement coefficients with spanwise accel. location.

Two primary observations may be made from this graph. The first is that the relative ratio between the two contributions from each component of acceleration approaches a constant as the spanwise location of the accelerometer increases. This would imply that two accelerometers located sufficiently far outboard would have trouble differentiating between inertial and centrifugal contributions of flapping in the signal. This is further illustrated in Figure 3.4, in which the ratio of inertial to centrifugal coefficients are plotted versus span location, and Figure 3.5, where the condition number of the matrix (a measure of its sensitivity to numeric perturbations) is plotted versus spanwise location of the *second* accelerometer, when the first is located at the 10% location for the above example.

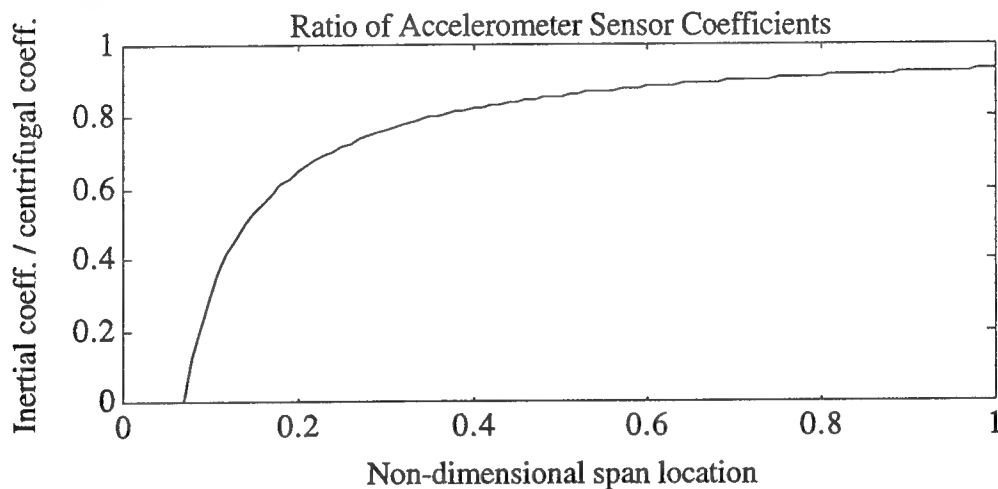


Figure 3.4: Ratio of flapping inertial to centrifugal contribution to accelerometer signal as a function of spanwise sensor location.

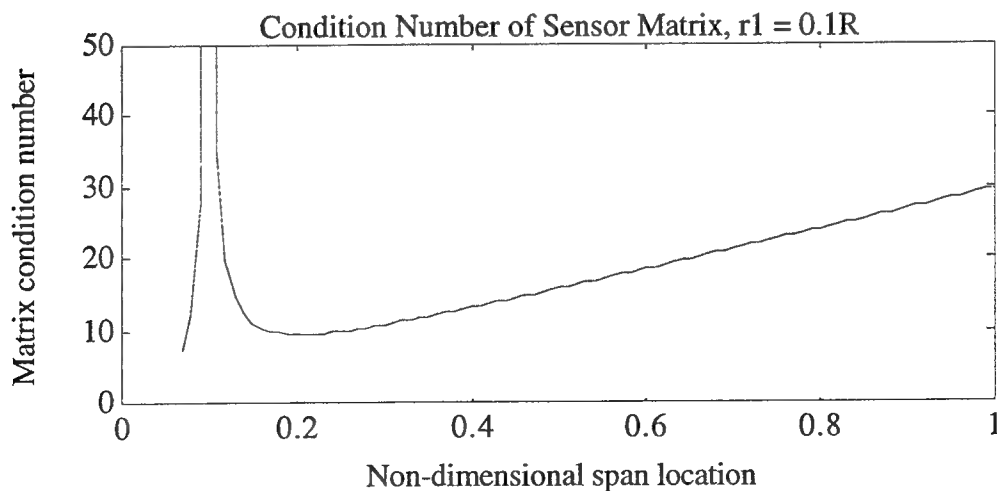


Figure 3.5: Matrix condition number versus spanwise location of second accelerometer, with first at 10% span position.

Figure 3.5 dramatically shows that the optimal location for the second accelerometer for this example would be exactly on the flapping hinge location at the 7% spanwise station. Were this not possible (and for an articulated rotor, this is likely), the next best location would be close to the 20% spanwise location. The condition number approaches and infinite value at $r_2 = 0.1R$, since we would have two sensors located on top of each other, thus generating a singular matrix in equation (3.9). Thus, this flap measurement technique is best served if the flap accelerometers are located *near the flapping hinge*. This is a fortunate results, as this location for the sensors would have the least adverse aerodynamic impact on the rotor system, they would operate in a modest centrifugal field, and impose the least requirements for cabling and electronic connections over any others.

Despite this good fortune, further examination of equation (3.9) and Figure 3.3 reveal that the measurement matrix is *singular* for the case of a centrally-hinged rotor system, such as common teetering rotors. In this case, $e=0$, which makes the relative contributions between the inertial and centrifugal acceleration components in the measurement matrix *identical*, regardless of sensor spanwise location. This apparent problem, however, may be overcome through consideration of the structure of a teetering rotor system. As shown in Figure 3.6 below, the rigid flapping dynamics of a teetering rotor system represents only a single degree of freedom, such that if two accelerometers are oriented as shown, with one located on the blade and the other above the teetering hinge, the inertial contribution will be in opposite directions, and thus the measurement matrix of equation (3.9) is once again invertable.

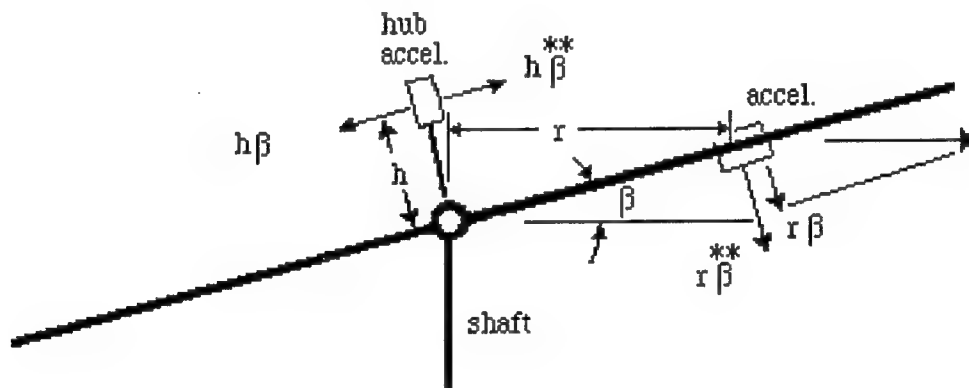


Figure 3.6: Accelerometer sensing schematic for teetering rotor

3.1.4 Hardware Realization Implications

The results of the above discussion show that the proposed accelerometer-based instrumentation scheme requires: (a) two transducers for each out-of-plane blade mode to be measured, at least one of which needs to be an accelerometer; (b) these accelerometers should be located fairly close to the hub (for blade flapping measurements), or hinge locations for articulated rotors; and (c) teetering (or gimbaled) rotor systems will require this instrumentation to be "divided" between the rotor blade and the hub in order to separate out-of-plane inertial effects from centrifugal acceleration effects for this type of rotor. These requirements are certainly not demanding, in that the amount of wiring, electronics and mounting hardware increases dramatically as the sensors are placed further outboard on the rotor span, due to the increased centrifugal loads encountered. From this fundamental basis, then, there appears to be no major impediment to the realization of an actual system for use in a flight test application.

3.1.5 Kinematic Observer Error Analysis

As shown in the preceding discussion, operation on the accelerometer sensors consists of solving n equations in n unknowns to determine modal acceleration and positions, and then using the double-integration-with-feedback scheme of the observer. Since there can be no error associated with modeling the kinematics (acceleration is a time derivative of velocity, which is a time derivative of a position), all the error that is introduced to the Kinematic Observer of equation (3.6) above comes from the errors associated with representation of the proper modal position and acceleration "measurement". Insight is provided, however, if one considers the filtering structure of the system represented by equation (3.6) through derivation of the transfer functions connecting the modal position and acceleration "measurement" with the observer estimates for modal position and velocity.

Taking the Laplace transformation of each side of equation (3.6) gives:

$$s \begin{Bmatrix} \hat{X}(s) \\ \hat{\dot{X}}(s) \end{Bmatrix} = \begin{bmatrix} -K_{11} & 1 \\ -K_{21} & 0 \end{bmatrix} \begin{Bmatrix} \hat{X}(s) \\ \hat{\dot{X}}(s) \end{Bmatrix} + \begin{bmatrix} K_{11} & 0 \\ K_{21} & 1 \end{bmatrix} \begin{Bmatrix} Y_1(s) \\ Y_2(s) \end{Bmatrix} \quad (3.10)$$

which after further simplification yields:

$$\begin{Bmatrix} \hat{X}(s) \\ \hat{\dot{X}}(s) \end{Bmatrix} = \begin{bmatrix} \frac{K_{11}s + K_{21}}{s^2 + K_{11}s + K_{21}} & \frac{1}{s^2 + K_{11}s + K_{21}} \\ \frac{K_{21}s}{s^2 + K_{11}s + K_{21}} & \frac{s + K_{11}}{s^2 + K_{11}s + K_{21}} \end{bmatrix} \begin{Bmatrix} Y_1(s) \\ Y_2(s) \end{Bmatrix} \quad (3.11)$$

Several observations are possible from the above expression. First, if y_1 truly represents a position measurement ($X(s)$), and y_2 represents a modal acceleration measurement ($s^2 X(s)$), then the blending of these two signals exactly yields the desired modal position and rate outputs. This combining of various derivatives associated with a physical quantity is sometimes referred to as a "complementary filter", and has most often been used in aircraft applications for blending angular rate and position measurements.

Second, errors associated with modal position measurements are transferred to the modal position estimate at unity gain at low frequencies, and are "rolled off" at high frequencies by a $1/s$ factor (i.e., the amplitude decreases with increasing frequency). Thus, bias errors associated with the modal position measurements would be diminished in predicting higher frequency modal responses. Modal position bias errors do not affect the modal rate estimate, since the (2,1) component in the above transfer function matrix is high-pass. Bias errors on the modal acceleration measurement, however, directly affect both position estimates (at low frequency by a $1/K_{21}$ factor) and modal rate estimates (by a factor of K_{11}/K_{21} at low frequency).

Third, all of the transfer functions relating the modal "measurements" to the estimated modal position and rate roll off at high frequencies. Thus, although in principle they could be "tuned" to have low break frequencies for providing additional filtering of higher-frequency "noise", maintaining proper signal-to-noise ratios on these same estimates would suggest that the filter break frequency be 3-5 times the natural frequency of the mode being observed for rapid tracking performance. Hence, the usual tradeoff exists in Kinematic Observer design that is present in all filtering schemes: one is forced to trade-off

filter transient performance with sensitivity to noisy measurement signals. Since the roll-off on the filters on the y_1 and y_2 measurements is at best only second-order, it has been found in previous investigations (and in the experiment described later) that additional pre-filtering of the accelerometer signals is necessary prior to processing with the observer structure above.

The net result, then, is that this signal processing scheme is most susceptible to error through the solution of the multiple sensor measurements in extracting the modal position and acceleration inputs to the Kinematic Observer. These sensitivities are further explored in the sections that follow.

3.2 Installation and Pre-Test Requirements

Since the measurement scheme involves the use of position-dependent accelerations for reconstructing the rotor blade motion and loads during flight testing, accurate *a priori* representation of the sensor location on the blade and its signal content is very important. This includes not only the knowledge of the sensor spanwise and chordwise position, but also the associated mode shape of the blade at the accelerometer location. The sensitivity of the measurements to errors in this position and modal representation in the sensor signal content is addressed in this section, and suggestions for various means to minimize its impact on the rotor motion and loads estimates are provided.

Close measurement of the physical *position* of blade-mounted accelerometers is not a difficult task. This may even be aided by providing specialized sensor "carriers" (discussed in more detail in the section on implementation issues below), that would position the sensors on a thin material that would then be bonded to the blade surface. However, what may be more difficult would be the determination of the various modal properties of a rotor blade, particularly for one that may have been used on an in-service aircraft for many flight hours. It would be most desirable to eliminate the necessity for removing the blade in order to perform a detailed shake or impact test. A possible means of providing this information is discussed below, but what is addressed here is that the determination of the modal properties will not be exact. This would have obvious consequences on the ability of a distributed set of sensors to separate the modal response variables, leading to errors associated with the representation of modal position and acceleration "measurements" that are fed into the Kinematic Observer.

Sensor location determines the values in the measurement sensitivity matrix that relates modal acceleration and position to sensor content. From Figure 1.2, for the out-of-plane orientation of k accelerometers, this becomes:

$$\begin{Bmatrix} accel_1 \\ accel_2 \\ \dots \\ accel_k \end{Bmatrix} = \begin{bmatrix} r_1 \Omega^2 \partial \eta_1(r_1) / \partial r & \eta_1(r_1) & \dots & \dots & r_1 \Omega^2 \partial \eta_i(r_1) / \partial r & \eta_i(r_1) \\ r_2 \Omega^2 \partial \eta_1(r_2) / \partial r & \eta_1(r_2) & \dots & \dots & r_2 \Omega^2 \partial \eta_i(r_2) / \partial r & \eta_i(r_2) \\ \dots & \dots & \dots & \dots & \dots & \dots \\ \dots & \dots & \dots & \dots & \dots & \dots \\ r_k \Omega^2 \partial \eta_1(r_k) / \partial r & \eta_1(r_k) & \dots & \dots & r_k \Omega^2 \partial \eta_i(r_k) / \partial r & \eta_i(r_k) \end{bmatrix} \begin{Bmatrix} q_1(t) \\ \ddot{q}_1(t) \\ \dots \\ q_i(t) \\ \ddot{q}_i(t) \end{Bmatrix} \quad (3.12)$$

for a truncated modal displacement series of i mode shapes.

Optimal sensor placement would not only minimize the condition number of the above sensor sensitivity matrix but also make *each term* in the matrix insensitive to minor variations in mode shapes for the rotor blade. Thus, it is of particular interest in the application of this measurement technique to determine where the accelerometers should be located on the blade. To gain an appreciation for this sensor location issue, the out-of-plane blade motion will be addressed. The approach taken here is to first minimize the condition number of the above matrix, for an increasing number of out-of-plane modes, and then to investigate the sensitivity of the matrix elements to variations in the representation of the mode shapes.

Although blade modal natural frequencies are known to vary significantly with rotor rotation speed, blade mode shapes are rather weak functions of this parameter (Ref. 42). The study in accelerometer placement here used *non*-rotating mode shapes for an offset hinge rotor, which are close approximations to those calculated for a UH-60A rotor blade (Ref. 50), the first three of which are shown in Figure 3.7. Sensors were added, two at a time, and distributed spanwise so as to reduce the condition number of the sensitivity matrix and thereby increase the signal-to-noise ratio of the generation of modal acceleration and position estimates. The most inboard accelerometer was limited to the 7% radius station to provide clearance for a blade grip and flapping hinge joint. The condition number of the resulting 2x2, 4x4 and 6x6 matrix, along with the associated optimized sensor locations, are shown in Table 3.1 below.

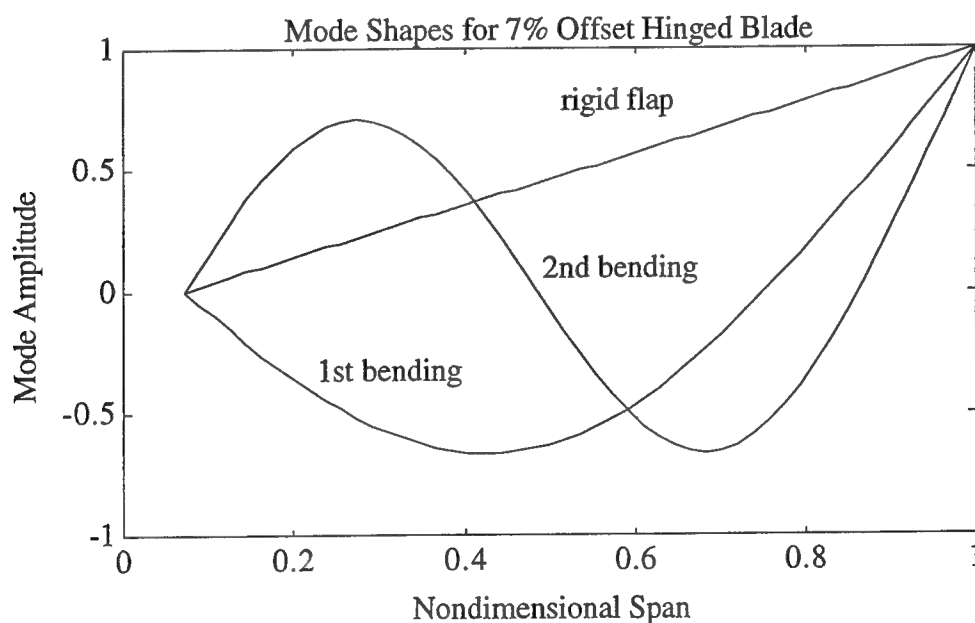


Figure 3.7: Out-of-plane mode shapes used in the optimization study.

Table 3.1: Optimum Sensor Locations as a Function of Modes Measured

| # Accels | Cond. Number | Modes Measured | Sensor Locations |
|----------|--------------|-------------------------------|--------------------------------|
| 2 | 5.82 | rigid flap | .07, .14 |
| 4 | 126.6 | rigid flap, 1st bending | .07, .373, .666, .949 |
| 6 | 3,704 | rigid flap, 1st & 2nd bending | .07, .177, .418, .67, .86, 1.0 |

Three observations may immediately be made from these results. First, as was shown in an earlier subsection, sensing of just rigid flap deflection for a rotor blade using this technique is best performed using sensors located near the flapping hinge (or equivalent). Second, as the number of desired modes is increased, the sensors "distribute themselves" along the blade span so as to maximize the combinations of bending slopes and displacement amplitudes to make the matrix of equation (3.12) as nonsingular as possible. And finally, the condition number of this sensitivity matrix, despite this attempt to minimize it through sensor placement, continues to degrade significantly with increased attempts to measure a larger number of modes.

Based upon this last observation, it was of interest to gauge the sensitivity of this matrix to small perturbations in individual sensor location. This was done by computing the matrix condition number as each sensor was varied individually away from its optimum location as computed above. The results, shown in Figures 3.8 and 3.9, indicate that, with the exception of the sensor located by the flapping hinge, the optimum sensor placement is not a very "sharp" minimum, and some latitude exists for locating these sensors at blade spanwise stations *near* these ideal positions.

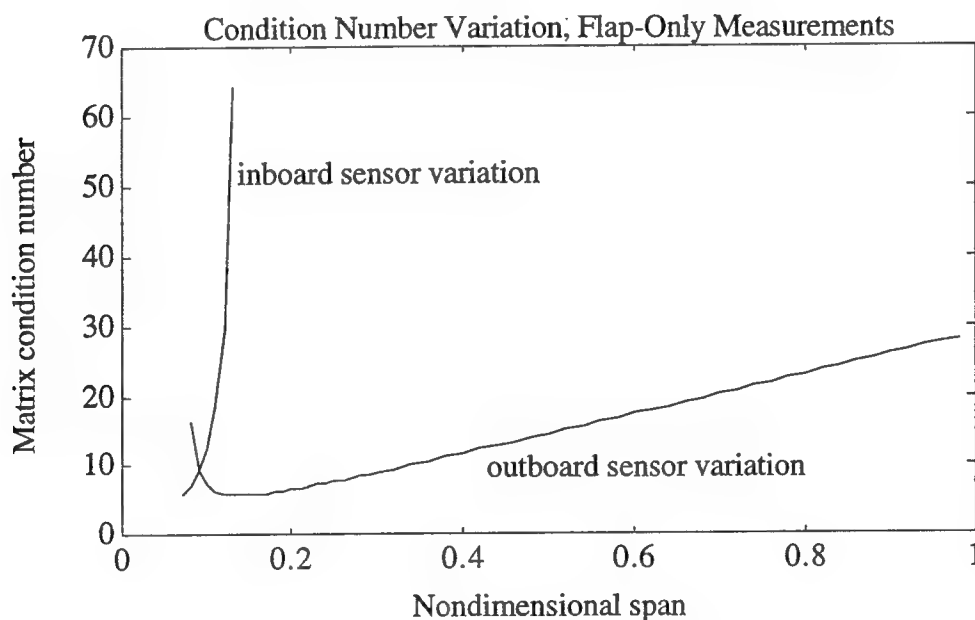


Figure 3.8: Variation in sensitivity matrix condition number with shifts in sensor location, two-sensor case (flap only measurements).

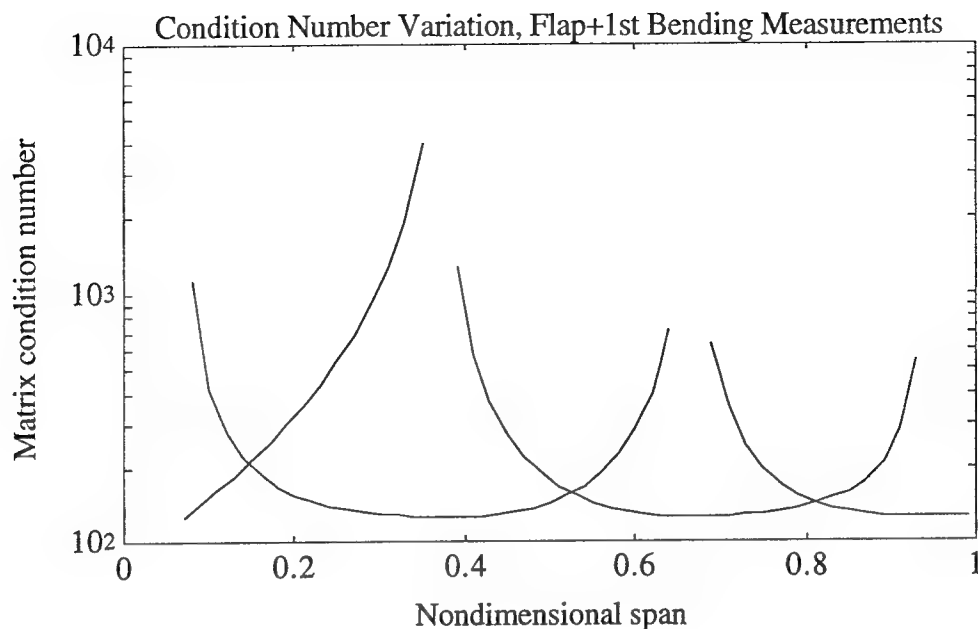


Figure 3.9: Variation in sensitivity matrix condition number with shifts in sensor location, four-sensor case (flap+1st bending measurements).

However, if these sensors are displaced from the optimum locations, and the original locations are used to compute the terms in the sensitivity matrix, the resultant blade modal motion and acceleration estimates suffer. As an example, the time-marching single-blade simulation was used to investigate the capability to re-generate modal position and acceleration measurements using spanwise mounted accelerometers, first with the accurate knowledge of both the sensor position and associated mode shape displacement and slope at that location, and then with the sensor displaced slightly but still using the same sensitivity matrix to reconstruct the modal response quantities. In order to more closely approximate reality, the simulation used four modes (rigid flap, rigid lag, first and second elastic out-of-plane bending), but only attempted to replicate two (rigid flap and first out-of-plane bending mode) using four out-of-plane accelerometers distributed spanwise. Thus, reconstruction of blade modal responses is not a trivial inverse problem, since the third out-of-plane modal response is neglected in the reconstruction process. Figure 3.10 shows that the reconstruction is quite accurate, when proper modal information is used, but suffers considerably, as shown in Figure 3.11, when the sensitivities used in the reconstruction differ from their actual values.

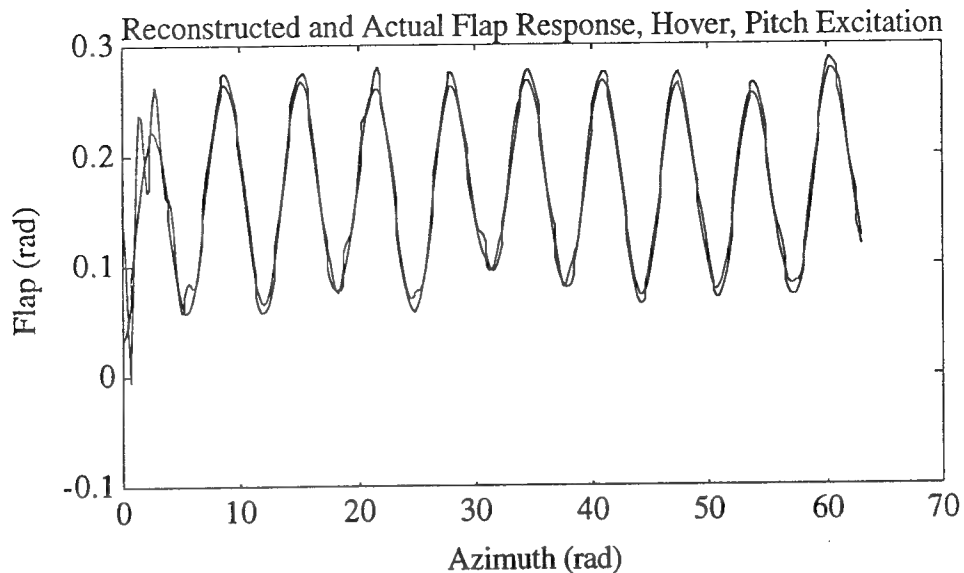


Figure 3.10: Reconstructed and actual flap mode displacement, using proper sensitivity matrix.

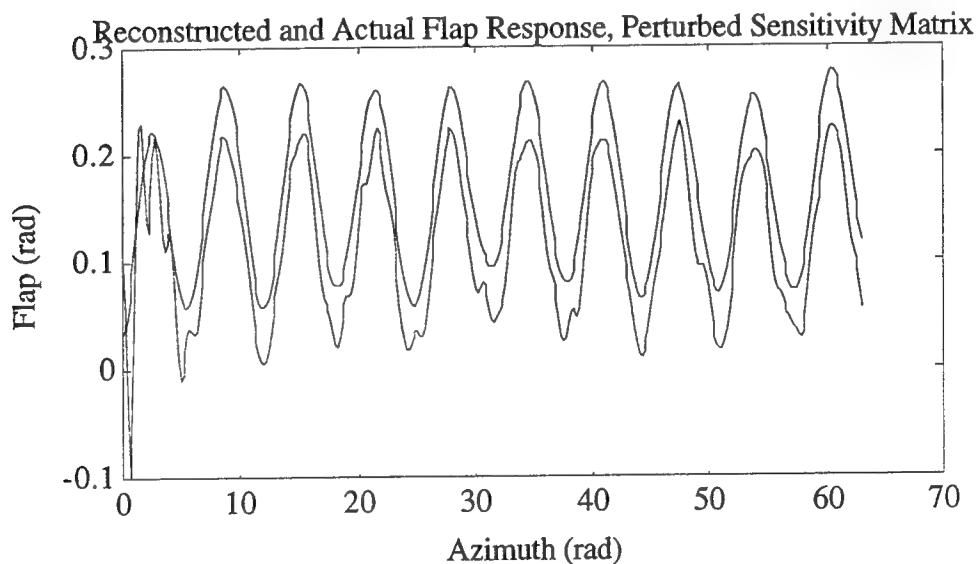


Figure 3.11: Reconstructed and actual flap mode displacement, using perturbed sensitivity matrix.

Part of this error may be attributed to the condition number of the sensitivity matrix, in that this value also indicates the sensitivity of changes in the linear equation solution to *variations in the matrix elements themselves*, not just noise sources on the sensors. As a means of helping address this problem, a novel hybrid sensor scheme was also investigated during this simulation study. If one considers the limiting case of bringing two out-of-plane accelerometers closer together on the blade, and measuring the *differential* acceleration between these two sensors, then one may formulate an expression for the difference in these two sensors when divided by the distance between them. This is,

effectively, a rotational accelerometer, which has been incorporated in commercial devices, such as the Kistler 8832 TAP (Translational/Angular Piezobeam) system. For applications in a rotational field, however, such a differential measurement provides a component due to centrifugal acceleration as well, as will be shown.

Considering the diagram of Figure 3.12, as the two accelerometers are brought together to within a distance ϵ of each other, the differential acceleration between the two is:

$$\ddot{z}(r_1 + \epsilon, t) - \ddot{z}(r_1, t) + (r_1 + \epsilon)\Omega^2 \frac{\partial z}{\partial r}(r_1 + \epsilon, t) - (r_1)\Omega^2 \frac{\partial z}{\partial r}(r_1, t) \quad (3.13)$$

If one now takes the limit as ϵ approaches zero, and divides this differential by this small distance, then the differential sensor will "see":

$$\frac{\partial \ddot{z}}{\partial r}(r_1, t) + \Omega^2 \frac{\partial z}{\partial r}(r_1, t) \quad (3.14)$$

where we have eliminated the second spatial differential of $z(r, t)$ since these two accelerometers would be mounted on a common, rigid carrier and *not* directly on the flexible blade.

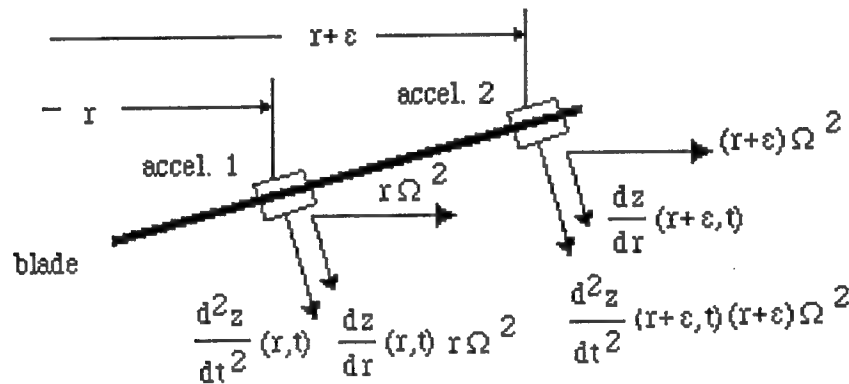


Figure 3.12: Schematic of hybrid accelerometer sensing unit.

Use of this differential measurement has several attractive properties. By co-locating two accelerometers at each spanwise station, the installation requirements for a particular number of sensors is halved. This means for a rigid flap measurement, only one hybrid accelerometer combination is required, to be located close inboard to the hub. In addition, measurement of this combination of acceleration and displacement *slopes* does not have a decreasing centrifugal component as the sensors are moved inboard, since there is no direct factor of "r" on this term. As a consequence, the matrix representing this hybrid sensor scheme does not exhibit the drastic increase in condition number with increasing sensors, as shown in Table 3.2 below.

Table 3.2: Optimum Sensor Locations as a Function of Modes Measured for Hybrid Average + Differential Acceleration Sensor

| # Units | Cond. Number | Modes Measured | Sensor Locations |
|---------|--------------|-------------------------------|------------------|
| 1 | 28.6 | rigid flap | .07 |
| 2 | 65.8 | rigid flap, 1st bending | .07, .356 |
| 3 | 96.2 | rigid flap, 1st & 2nd bending | .194, .236, .750 |

Another advantage of this hybrid sensor is that, at zero rotation speed, these sensors not only sense displacement accelerations, but also slope accelerations as well; this combination of both displacement and slope information, at zero rotor rotation speed, would allow for better pre-test modal identification of the blade prior to the use of the instrumentation in flight test.

Confirmation of this improvement in sensitivity matrix conditioning comes from additional exercises where this hybrid scheme was used to again reconstruct flapping motion from simulation data. Reconstruction of flapping is actually *improved* over the previous scheme when the proper sensitivity matrix is used in the equation solution process, as shown in Figure 3.13. When similar perturbations are made to the sensitivity matrix as for the previous case, the reconstructed flapping motion is degraded (shown in Figure 3.14), but not as severely as the previous, single-accelerometer-sensor example above.

Although this improved measuring scheme using co-located dual accelerometers shows improved results, the experiment described in the next section used individual accelerometer sensors, due to the pre-existing blade that had accelerometers already installed in this manner.

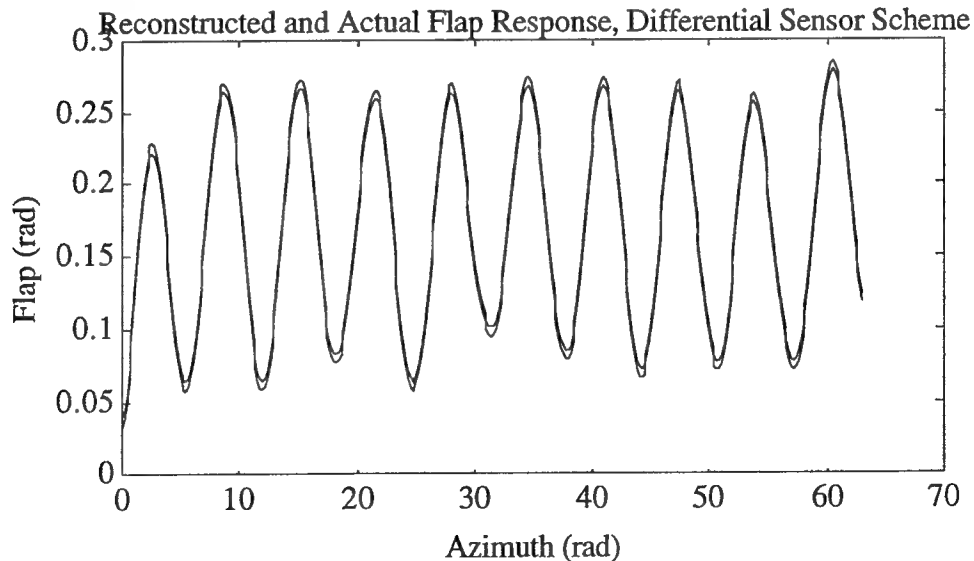


Figure 3.13: Reconstructed and actual flap mode displacement, using differential accelerometer sensors.

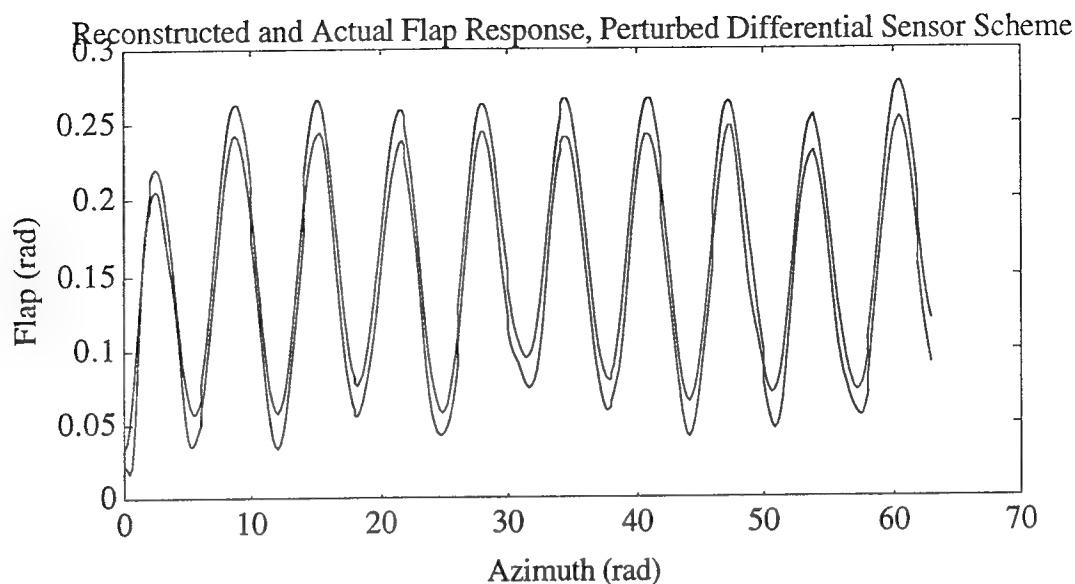


Figure 3.14: Reconstructed and actual flap mode displacement, using perturbed sensitivity matrix and differential accelerometer sensors.

3.3 Adjustment of Instrumentation System Bandwidth

While high levels of Kinematic Observer feedback gain may improve the transient performance of the tracking of rotor blade motion, it can also compound errors in estimating higher modes of rotor response. This is due to the phenomenon known as "measurement spillover" (Ref. 49), where effects from higher frequency modal responses can infiltrate and corrupt measurements that have not properly included (or completely ignored) their effects in the analytical representation of the sensor output. Thus, a balance must be found between tracking (transient) performance and apparent "noise" introduced from the sensors themselves.

As was shown in the previous section, however, the transfer function of the Kinematic Observer relating accelerometer sensor inputs to modal displacement and velocity estimates has only a second-order denominator in the Laplace variable, indicating that the suppression of higher frequency accelerations is only attenuated at a -40dB/decade rate. This is not a very sharp roll-off when one considers that the modes of interest on a helicopter tend to fall within integer numbers of themselves, as opposed to being separated by orders of magnitude. Thus, pre-filtering of the accelerometers is an absolute requirement in practice, as is shown in the section that follows where the model rotor experiments are described. Choice of Kinematic Observer bread frequency has typically used only a factor of three over the natural frequency of the mode being observed, and this rule of thumb was followed in the experiment described later.

3.4 Sensitivity to Sensor Errors

Accelerometer sensors may be subject to drift over time, shifts in gain due to temperature effects, and may have an unknown bias present arising from manufacturing tolerances. In addition, the signal processing hardware, such as an A/D converter, may introduce errors in the measurement as well. Suggested methods for either accommodating these or minimizing them would include: initial bias removal during power-up sequence,

on-sensor temperature accommodation (typically supplied with commercial units), and periodic re-zeroing of the sensors by incorporating a bias "state" along with each measurement. Again, this latter option is only available if a measurement exists that provides an un-biased slope or displacement measurement. This could perhaps imply that a "zero-drift" accelerometer is used at the reference sensor, and all others include a bias state in the estimation of the modal quantities measured at these other spanwise stations.

A/D conversion errors are typically not a driving concern, provided that the amplifiers that boost the accelerometer's signal are scaled properly to use a significant portion of the range of the A/D converter's input capabilities. Commercial multi-input, serial digital output devices are now commonplace (see, e.g., the system constructed in Ref. 33), often with 10 to 12 bits of resolution. This error source will be significantly lower than any associated with proper modal shape identification for the instrumented blade.

3.5 Self-Calibration and Self-Test

Advanced instrumentation should include some self-diagnostic capability to assist the test engineer in the production of a successful set of test data. More recent sensor developments have begun to include self-test capabilities, such as the Analog Devices ADXL50 capacitive accelerometer (Ref. 63). This device provides a pin whereby an applied voltage generates a deflection of the active member within the accelerometer, providing both substantiation of a working device, and a means of an approximate calibration at the same time.

Self-calibration of an installed sensor suite on a rotor blade would greatly aid the flight test engineer. While not attempted during this Phase-I investigation, a promising potential technique for self calibrating the modal sensitivity matrix associated with an installation may be as simple as selecting a "self-test" mode on the measurement device, and then performing a crude "twang" test on the instrumented rotor system by deflecting the blade structure by hand, and then letting the blade "ring down", providing measurements of its non-rotating natural frequencies and modal displacements. These accelerometer signals recorded during this non-rotating pre-flight would, using the hybrid unit described above, provide both modal displacements and modal slopes at each sensor location, aiding the identification (or pre-test calculation) of the blade modes for subsequent extraction from the flight data. These identified modes could be corrected for shape changes to correspond to a nominal rotation frequency, or left alone, since the modal shapes are only weak functions of centrifugal stiffening. This concept is proposed for investigation as part of the follow-on work to this investigation.

3.6 Reconstruction of Rotor Loads

While measurement of rotor motion is of paramount importance in the proposed measurement system, it is also of considerable interest to investigate the capability of using the resulting data for determining rotor loading information. Determination of rotor loads from the identified modal response of the blade is not unlike the approach used in the Strain Pattern Analysis (SPA) method (Ref. 21), where the knowledge of the structural response (measured using strain gauges) is used to determine both the blade inertial and aerodynamic loads - *but data from this measurement technique provides an important difference*. To appreciate this difference, one need only consider the blade out-of-plane bending equation, which relates the second spatial derivative of the structural moment to the applied inertial and aerodynamic load according to:

$$(EIw'')'' = (Tw')' - m \frac{\partial^2 w}{\partial t^2} + F_{Z_{AERO}} \quad (3.15)$$

The SPA approach uses identified strain patterns to determine both blade elastic deflections and structural bending moments. These constitute the first term on the right and left sides of the above equation. Then, these loadings are separated into frequency components, with simple harmonic motion assumed at each integer multiple of rotor rotational frequency, in order to determine the inertial loadings on the rotor (the second term on the right of equation (3.15)). Thus, algebra provides the air loading term, which would represent a linear combination of the modal forcing functions, for all the assumed modes participating in the response. Put in other terms, the identified airload is represented by basis functions that are in fact the blade natural mode shapes, and thus the larger the number of modes included in the analysis, the more spanwise (spatial) resolution possible in the determination of this loading. In addition, by using the assumption of forced response at integral multiples of rotor rotation frequency, this method allows for *steady, periodic* determination of both inertial and aerodynamic loads from measured structural response.

The primary difference of the SPA approach and the one employed here, is that not only blade modal displacement response is made available from the measurements, but also blade modal *accelerations*. This added measurement means that one *does not have to assume simple harmonic motion* in representing the inertial loading on the blade, and hence, measurement of transient aerodynamic loading is possible. This capability can only be *approximated* using the SPA approach. Thus, use of this measurement methodology allows tracking loads during transient maneuvers, something greatly desirable in a flight test program.

By means of illustration, the initial transient portion of the simulation described in the previous subsection is used to compare the applied airload on the rotor with reconstructed airloads using identified modal responses and accelerations. Figure 3.15 shows a surface plot of the airload in the simulation during the initial transient response, and Figures 3.16 and 3.17 show this same airload reconstructed using various combinations of the measured modal displacements and accelerations. When all three out-of-plane modes are used, the reconstructed airload is remarkably similar to the applied loading, whereas when only the flap mode is used, the airload distribution is adequate for handling qualities-type investigations, but probably not suitable for calculating vibratory loads on this rotor. Of particular interest in both 3.16 and 3.17 is the excellent fashion in which the transient is captured, *something extremely difficult to obtain using any other approach*.

An observation from the above simulation study shows that this technique is indeed quite promising, and should be quantified in future work using a detailed data set, as is discussed in the section on follow-on investigations.

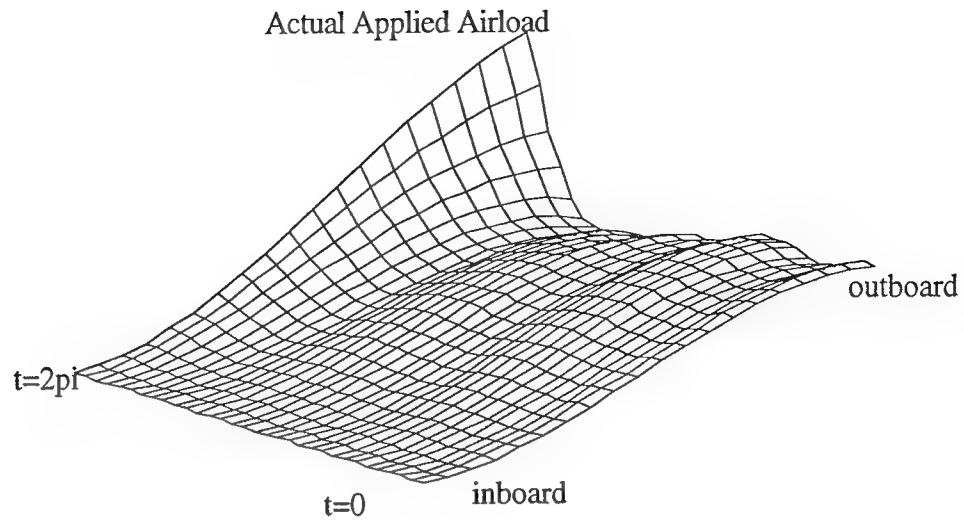


Figure 3.15: Applied airload during initial simulation transient.

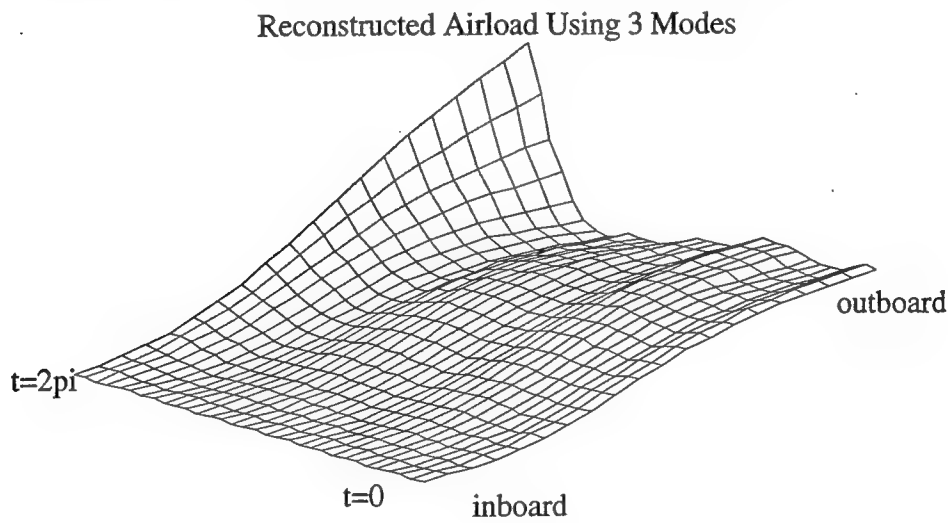


Figure 3.16: Reconstructed transient airload using all out-of-plane mode shapes.

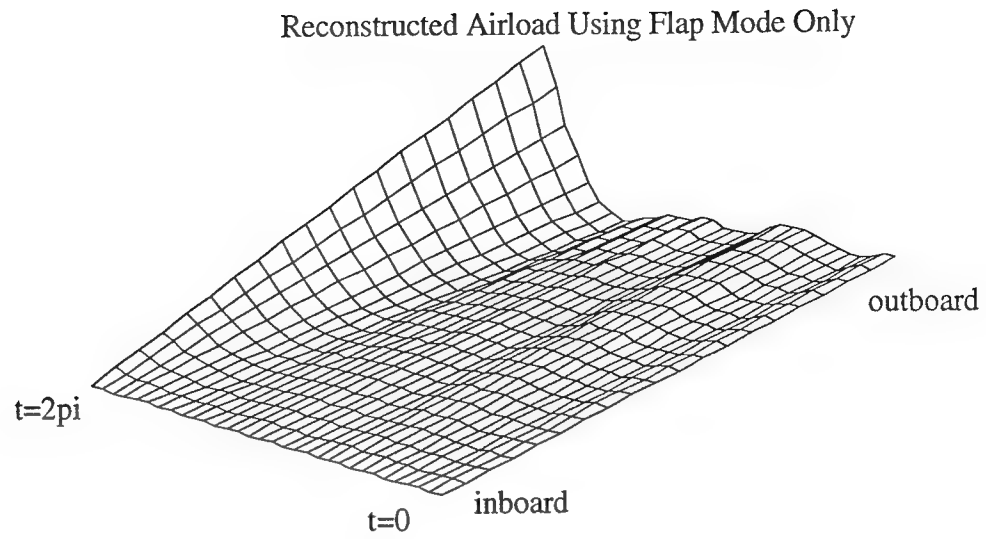


Figure 3.17: Reconstructed transient airload, using only the flap mode shape.

4.0 HARDWARE DEMONSTRATION

4.1 Description of Model Demonstration Hardware

The primary goal of this portion of the Phase-I investigation was to validate, in a restricted sense, the approach for measuring rotor motion using an actual experimental rotor system. The validation would come from direct comparisons between rotor flapping measurements estimated from the accelerometer-based measurement scheme, and those from a discrete sensor (potentiometer) mounted on a flap hinge. Previous work done by the Principal Investigator on sponsored research projects at Princeton University provided access to a range of model rotor system hardware for use in supporting this effort. While these models include both hingeless and gimbaled rotor hub configurations, none of them had been built with discrete hinge locations that could readily accommodate a potentiometer or similar rotary motion transducer. Thus, while blades, grips, swashplates and the like were borrowed from these various systems, a new hub system had to be designed and built to support the needs of the qualification of the proposed measurement scheme.

Most of this rotor hardware incorporates components from radio-controlled helicopter kit parts, and thus, is designed for reduced Mach number model testing. While such models may not provide adequate representations for helicopter performance testing, the primary purpose of the measurement scheme is to accurately reconstruct rotor blade motion and loads, and thus these quantities need only be representative of those on a full-sized aircraft. It was decided at an early point, then, to use a Froude-scaled model rotor as a demonstration and development platform. Froude-scaling provides for the proper vectorial representation of the various specific forces (accelerations) on an object, which is particularly important for a scheme that uses direct acceleration measurement in its signal processing scheme. An additional advantage of the choice of Froude scaling is that the stresses in the model components are quite reasonable, versus having to design to full-scale stresses for a Mach-scaled model rotor system. Power requirements for Froude-scaled rotor systems are also modest, such that the 4-foot diameter model rotor tested only required a 1 HP dc motor. A photograph of the model rotor and fuselage attached to a support sting is in Figure 4.1.

The hinge sequence for the model rotor hub is (from the hub centerline outboard): flap, then pitch, then lag, thus providing a sufficiently challenging sensing requirement for the accelerometer-based device. The flap hinge was instrumented with a single-turn potentiometer connected directly to the hinge joint, the pitch angle was sensed using a single-turn potentiometer geared to a curved rack attached to the blade grip, and the lag motion was uninstrumented. Past experience with these model hubs indicates that since lag motion is heavily damped through friction (controlled by lag pin tension), lag displacements are quite small. A photograph of the rotor hub and the potentiometers is in Figure 4.2.

On-blade measurements were provided from four spanwise-mounted accelerometers oriented in the out-of-plane direction. These accelerometers (Entran Devices EGA-125D) had been previously installed in a Froude-scaled blade used in experiments described in Ref. 29. The untwisted, untapered blade also had two accelerometers oriented to measure in-plane accelerations, but these were not used in the experiment due to limitations on the number of slipring channels on the rotor shaft. The out-of-plane accelerometers were located (nominally) at 30%, 50%, 70% and 90% of blade span, at the 25% chord location of the rotor blade to minimize contamination of their signals with pitch accelerations. A sketch of the blade and the accelerometer locations is given in Figure 4.3.



Figure 4.1: Froude-scaled model rotor on test stand.

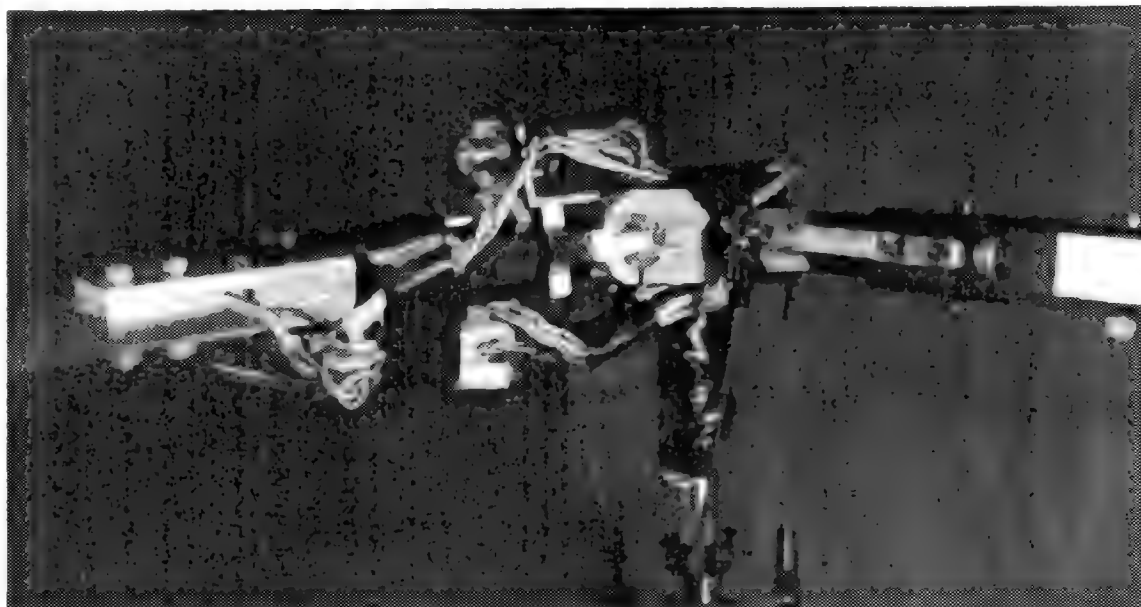


Figure 4.2: Instrumented model rotor hub with pitch and flap potentiometers.

The use of four accelerometers would potentially allow the measurement of two out-of-plane modes for the rotor blade, but since only the root flapping hinge was instrumented (and not any surface strain gauges on the blade), the only point of comparison for the demonstration experiment was the flapping estimate. Future experiments would ideally include additional instrumentation (such as surface-mounted strain gauges) for providing validation of elastic modal responses. The use of a Froude-scaled blade, however, provides added realism to the experiment in that the elastic mode frequencies are in the same approximate ratios to rotor rotation frequency as would be found on a full-size rotor blade. The accelerometers will thus have additional signal components due to higher frequency modal response, and thus provide a realistic test environment that would simulate the challenges of an actual flap-only sensing scheme on a flight test aircraft.

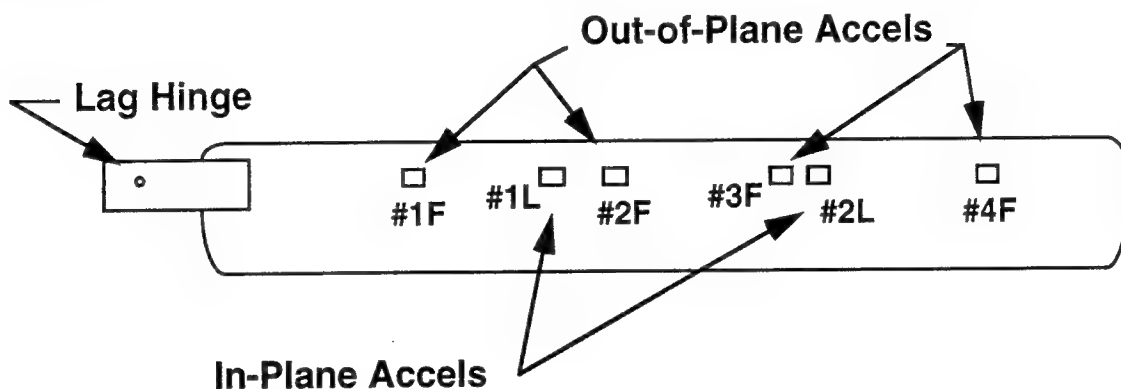


Figure 4.3: Schematic of instrumented rotor blade accelerometer locations.

During testing of the rotor all out-of-plane acceleration signals were recorded, although for some estimation exercises only the two inboard out-of-plane accelerations and the discrete flap hinge potentiometer were used in the comparison exercise. Operation of the rotor was performed indoors in hover for a range of collective settings, with rotor cyclic "stirring" used to excite blade flapping motion to provide a rich set of dynamic data for correlation purposes. Although significant rotor wake recirculation was present, the primary interest in comparison of flap acceleration-based estimates with flap angular position measurements is not affected by this adverse rotor operating environment.

The rotor and drive system assembly was mounted to a six-component strain gauge sting balance, and thrust loads were recorded in concert with the rotating-frame data, in hopes of providing additional data for comparison of inferred rotor loads with measured loads data. Due to electronic problems with the balance assembly, however, this data was deemed sufficiently unreliable and was not included for analysis as part of this experiment.

4.2 Scope of Tests

As mentioned above, the hover testing was performed indoors with manual swashplate "stirring", so as to excite significant blade transient flapping response in the model rotor. This was to provide a set of data that would contain unsteady flap (and elastic bending) response data that would be typical of an aggressive flight testing program on a full-size rotary wing aircraft. The rotor operating speed was nominally 300 rpm, and each channel of data was sampled at a per-channel rate of 256 Hz. With 512 points per channel, this provided a full two seconds of data for each channel per run, or approximately 10 rotor revolutions. Several runs were taken in series, along with a beginning run zero and end run zero point to assess any potential drifts in the accelerometer sensor measurements.

Filtering of the accelerometer signals was applied prior to digitizing by the A/D converter, using a bank of switched capacitor filters driven with the same clock input. Use of a common clock guaranteed that these filters would all exhibit the same magnitude and phase characteristics across the various accelerometer channels. Processing of the test data included an investigation of various filtering bandwidths, in both a pre-processing filter, and in the design of the Kinematic Observer, in order to determine the best means of trading off tracking performance with sensitivity to higher modal "noise" in the measurement estimates.

4.3 Hover Response Comparisons

The purpose of this demonstration test was to verify the technique of using distributed accelerometer measurements to reconstruct blade modal response. The demonstration was limited to only providing a potentiometer measuring flapping hinge rotation, and thus, all the comparisons shown below concentrate on reconstruction of the flapping measurement using only accelerometer signals. An average value of the beginning and end run zero points were used to remove potential bias signals from the accelerometer measurements, and then these filtered accelerometer channels were fed into a Kinematic Observer with a break frequency of $3\times$ rotor rotational speed to reconstruct blade flapping measurements. As can be seen in Figure 4.4, the reconstructed flap measurement compares quite favorably with the measurement from the hub-mounted potentiometer at the flapping hinge. The offset between the two signals shows that the averaged beginning and end run zero points correspond to the blade resting on its flapping stops, which corresponds to approximately 10 degrees of droop, which represents the difference between the two curves. Since four spanwise accelerometers were available for out-of-plane measurements, and only two were required (theoretically) to measure the flapping response, a least-squares fit of the sensitivity matrix relating these four sensors to the flap acceleration and position was used in the generation of the input "measurements" to the Kinematic Observer that provided the trace in Figure 4.4. This technique is useful for sensing lower frequency modes when additional instrumentation is available, and is performed on a regular basis in applications of Strain Pattern Analysis.

To reinforce the fact that prefiltering of the accelerometer signals is desirable, Figure 4.5 below shows what can happen if the only filtering is that of the second-order roll-off inherent in the Kinematic Observer. The estimated flap signal shows significant contamination of measured responses from higher bending modes, and would be unacceptable for any rotor measurement use.

Finally, if only the two most inboard accelerometers are used in the reconstruction of the flapping estimate, the results of Figure 4.6 are produced. This shows the disadvantage of using blade span locations for measurements that are not optimized for this reconstruction: the accelerometers were located at 31% and 50% of rotor radius, far from the hub and the flapping hinge point. These locations were already established for this rotor from a previous experiment, and since the model blade was readily available (and difficult to re-instrument), these locations were "accepted" for this demonstration test. Follow-on work would, of course, use locations closer in to the hub to reflect the analysis above that shows this to be a more desirable location for flap measurement sensors.

The high frequency influence of these higher modes on the anomalous behavior shown of the off-design cases above is readily apparent in Figures 4.7 and 4.8, showing both the raw accelerometer signals and the pitch, flap, and rotor pulse channels for the experiment.

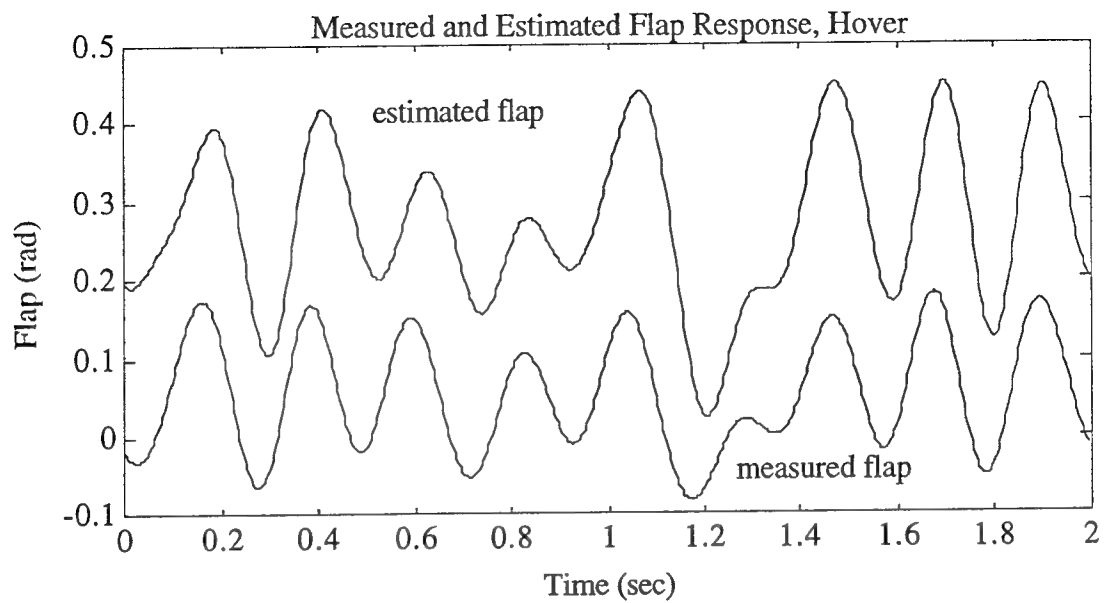


Figure 4.4: Comparison of blade flap measurement and Kinematic Observer "flap" output, hover.

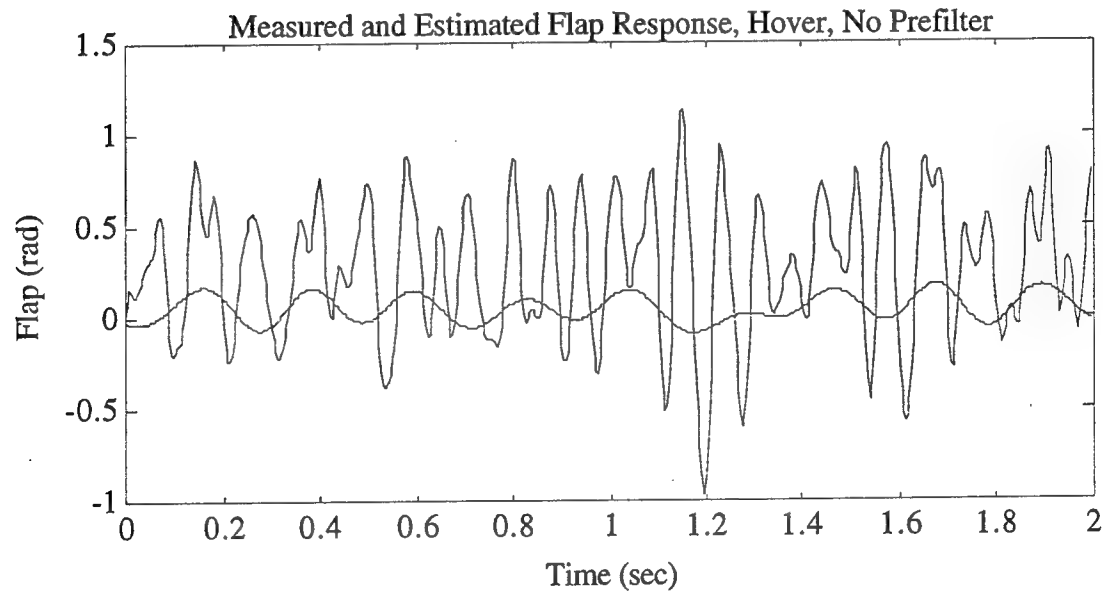


Figure 4.5: Comparison of blade flap measurement and Kinematic Observer output, hover, without accelerometer prefilter.

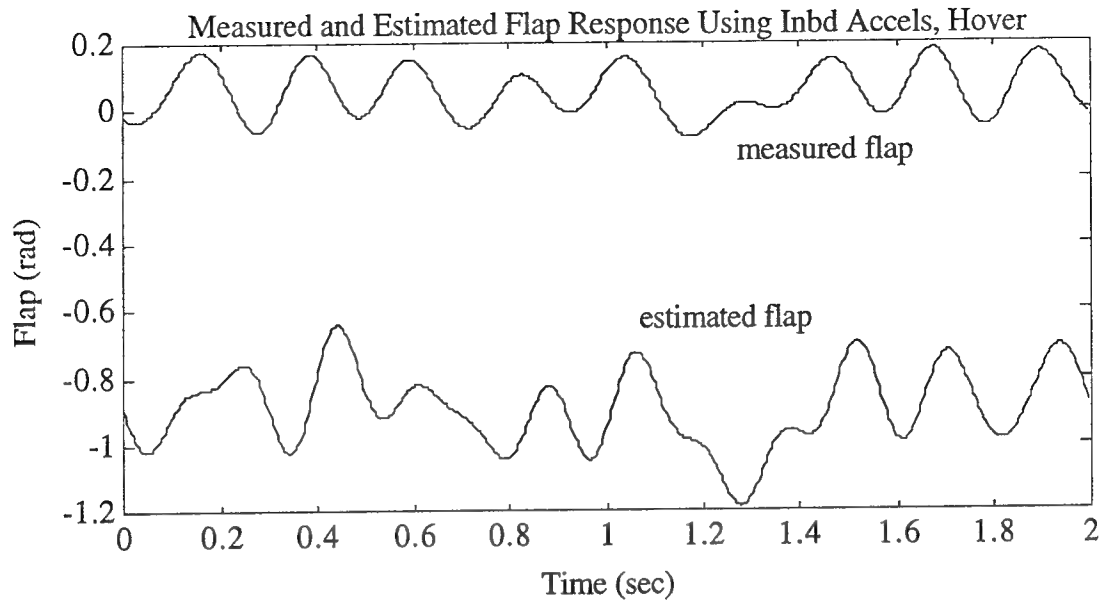


Figure 4.6: Comparison of measured and estimated flap response using only inboard accelerometers at 31% and 50% span.

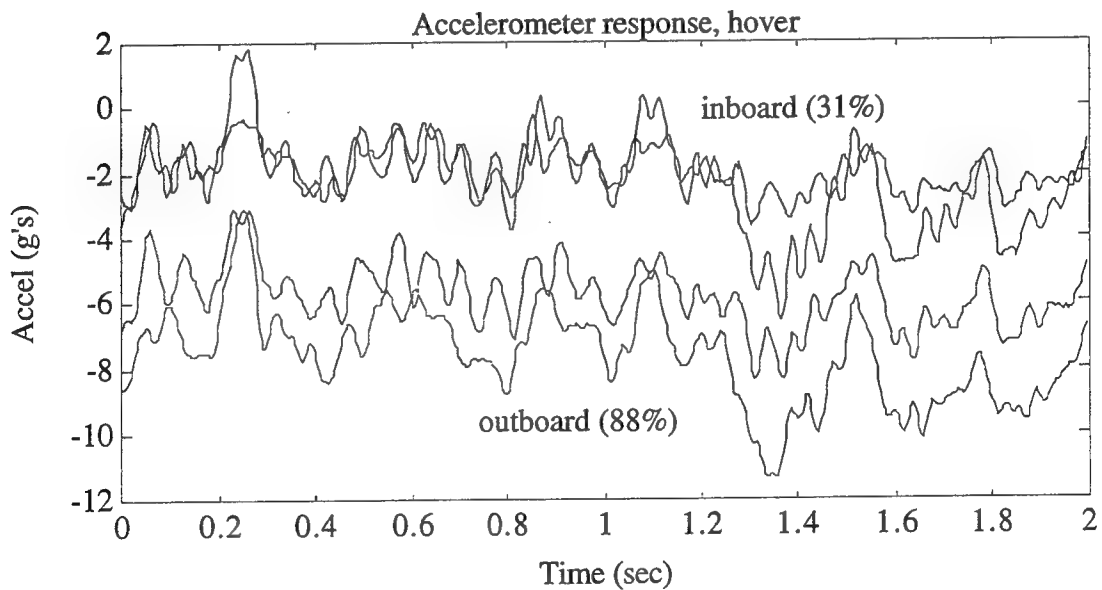


Figure 4.7: Model rotor accelerometer response, hover.

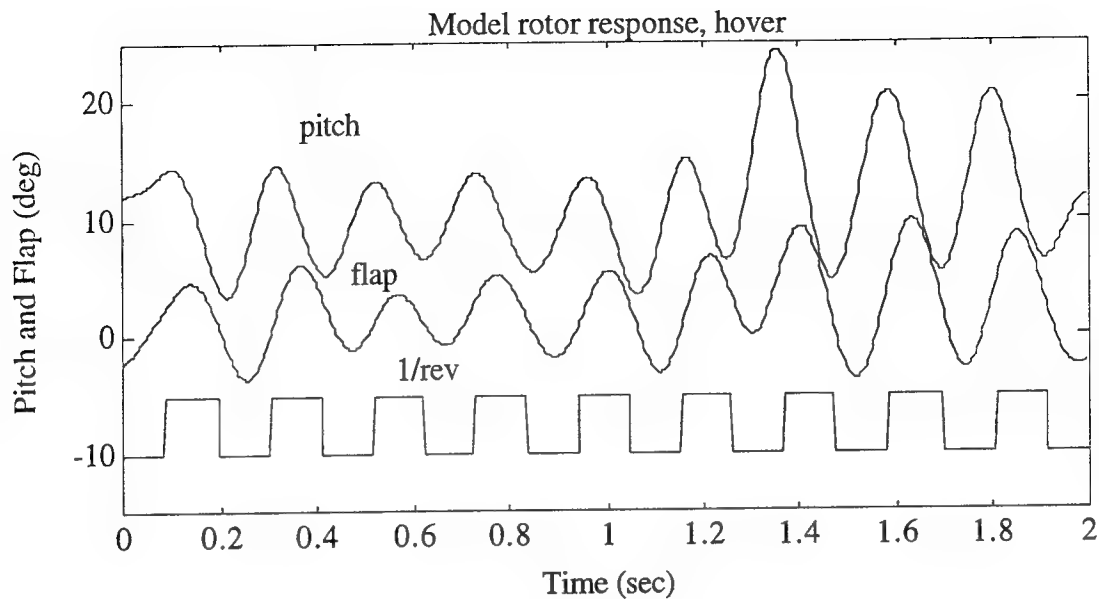


Figure 4.8: Model rotor pitch, flap, and 1/rev response, hover.

The net result from the demonstration testing showed, *for the first time*, a direct comparison of rotor flapping motion measured from a hub-mounted potentiometer and a series of distributed blade-mounted accelerometers, thus vindicating the approach for this measurement technique. Further testing of this system for comparisons with strain gauge data (for higher modal response checks) and for other rotor hub configurations is warranted; suggested methods for extending this experimental program are described in later sections of this report.

5.0 IMPLEMENTATION ISSUES

A limited study of implementation issues was addressed as part of this Phase-I study, although this component of research would be completely addressed as part of a Phase-II follow-on research topic. The goal of the study here was to attempt to identify any potential problem areas associated with implementation that may impose a severe impediment to an attempt to convert the concept to prototype hardware. The issues addressed included selection of sensor hardware (and consideration of alternate, non-accelerometer sensors), signal conditioning and scaling requirements, signal transmission from the rotating frame to the fixed fuselage frame (particularly telemetry systems), subsequent signal processing, and means of data storage and archiving for post-test analysis. In addition, issues of measurement system power and installation and removal are touched upon briefly.

5.1 Sensor Technologies

Although the focus of the effort here has involved the use of accelerometers *exclusively* in the determination of both rotor motion and loads, alternate sensors could conceptually be included in the instrumentation device to provide additional position or rate information. This capability is a consequence of the Kinematic Observer's use of only blade kinematic relations in its representation of the rotor system dynamics, and thus, the blending of additional blade modal rate or position measurements is a trivial exercise. This was in fact done in Ref. 13, where a rotor blade tip accelerometer was used in concert with a strain-gauge instrumented hub flexure that provided flap position information. It is thus appropriate to review potential sensor technologies that may provide an added benefit to this rotor motion and loads measurement task.

Since one of the primary goals of the instrumentation system proposed here is to make the device sufficiently aircraft-independent so as to *avoid* the need to accommodate discrete hinge joints (when they exist) on the rotor hub, only non-contact sensors will be considered for discussion here. That is, any device that requires a physical connection between two attachment points and senses the relative motion between them is not deemed sufficiently general for consideration. These include, for example, potentiometers, LVDT or RVDT (induction coil-based) devices, or instrumented linkages (such as the Sikorsky "crab arm", Ref. 23) that attach to both the blade (or blade grip) and the hub. Suitable non-contact sensor technologies would thus include: optical position measurement devices (e.g., lasers, video units, or LEDs), ultrasonic and acoustic position sensors, magnetic proximity detectors, capacitance-based position probes, RF-based units (such as GPS patch antennas), and inertial measurement devices, which would include the accelerometer-based scheme investigated here.

5.1.1 Optical Units

Optical detection units are, of this writing, still being investigated as one of two technologies for incorporation on NASA Ames' RASCAL UH-60A test aircraft (the other being an accelerometer-based scheme, Ref. 50). The laser-based method uses a hub-mounted laser to illuminate a reflective target located on the rotor blade, and processes the reflected beam for sensing the angular deflection of the blade relative to the rotor hub. A similar approach is being studied by researchers at the University of York (Ref. 51), although the details of that work have not yet been published. Advantages of the technique include an extremely wide bandwidth and fine resolution of motion; disadvantages include the requirement for laser system "hard points" on the rotor hub, limited operation in

inclement weather, and the susceptibility of the device to hub vibrations, since the relative motion may be produced by either hub or blade displacements.

A recent SBIR Phase-I program investigated the use of video units to determine rotor blade position (Ref. 52), but it is not apparent that this technology has reached a stage of sophistication to measure elastic rotor blade response as well. Conventional video systems also require sufficient ambient light levels for proper operation, limiting their use in certain flight testing.

Finally, LED-based devices have been used in numerous applications for angle resolution and in object detection (e.g., Ref. 53), but the separation distances typically found on rotorcraft hubs and blades would require rather high power levels to achieve reasonable signal-to-noise levels for such systems.

5.1.2 Ultrasonic and Acoustic Units

Ultrasonic sensors provide a nonintrusive means of measuring position of objects over moderate distances (up to typically 20 feet), and have been most successfully used in auto-ranging applications for instant camera focus adjustment (Ref. 54). Combination of ultrasonic / acoustic devices allow for two and three-dimensional position detection, with applications including three-dimensional digitizing (Ref. 55) and head tracking for helmet-mounted displays (Ref. 56). These devices typically do not require mounting targets, since the reflected acoustic energy is typically available from the sensed object at close to right angles. For rotor blade sensing, however, conventional application of this technology would be difficult, as the planar orientation of the blade, relative to the hub, would provide only a weak return signal to the acoustic detector, and thus some target would probably be required for mounting on the blade (assuming the acoustic source is located on the hub).

5.1.3 Magnetic Proximity Detectors

These devices operate on the principle that magnetic fields may be sensed using Hall-effect devices, or eddy currents may be induced in ferrous materials, thereby altering magnetic field strength or orientation. Thus, either ferrous material is required for a target or the sensed object, or magnets must be mounted opposite to the detector unit. Since composite rotor blades are becoming more prevalent, some form of supplied target is required. The primary difficulty with these detectors is their operating range, which at best is only a few inches. Application to elastic blade deflection measurement would thus be quite difficult.

5.1.4 Capacitive Probes

Variation in dielectric constant between capacitive plates (or similar geometries), induced by the proximity or intrusion of an object or target, will change the capacitance of these devices and thus alter their phase response in a coupled electrical circuit. These units have the advantage that they may work with a variety of materials, but suffer from similar limitations in distance of operation.

5.1.6 RF Based Systems

Use of radio-frequency (RF) phase change characteristics, such as incorporation of GPS signals with a "pseudolite" GPS transmitter, has been suggested for rotorcraft applications (Ref. 57), but problems with speed of update for this concept have yet to be addressed. This technique has been demonstrated for spinning spacecraft attitude determination, but conventional rotor rotation speeds are significantly higher. This concept

is at a very early stage of investigation, and would need further study prior to any incorporation with the measurement scheme proposed here.

5.1.7 Inertial Measurement Units

This category includes any device sensitive to inertial loading, and covers not only accelerometers, but tilt sensors, inclinometers, and miniature gyros. Tilt sensors typically use a fluid medium that reorients its free surface within a volume to determine local "level" orientation. Speed of response is typically governed by the settling time of the internal fluid, which is on the order of 500 ms, and thus, too slow for rotor blade angular orientation sensing applications (Ref. 58). Inclinometers are often servoed accelerometers, and thus have bandwidths limited by the internal servo system used for self-leveling; these units thus suffer from similar limitations for the present application.

Miniature gyros are available using vibrating quartz tuning forks (Ref. 59) or piezo-ceramic vibrators attached to a prism (Ref. 60) that have impressive drift rates and performance figures. These units would be capable of measuring angular rates at localized blade span locations, such that for an out-of-plane blade displacement $z(r,t)$ and an in-plane displacement $y(r,t)$, the gyro could measure $\partial \dot{z}(r,t) / \partial r$ and $\partial \dot{y}(r,t) / \partial r$ respectively. The difficulty with attempting to measure in-plane rate in this fashion would come from the fact that the sensor would be nominally aligned with the rotor rotation vector and thus two gyro sensors would most likely be necessary in order to subtract out the (somewhat) steady rate signal associated with rotor rotation. An additional difficulty is that as the blade's pitch angle is changed, this same rotor blade rotation rate would be sensed by the out-of-plane rate sensor, in a level proportional to the sine of the pitch angle. Since pitch angle of a rotor blade is the same order of magnitude as its flap angle, and since the dominant vertical velocity is due to 1/rev flapping, then it would be difficult indeed to sort out contributions of $\theta\Omega$ and $\dot{\beta}$ in these measurements. For this reason, use of "chip"-based vibrating gyro sensors is probably not practical for this application.

Finally, it is important to understand the requirements placed on the accelerometers to be used in this measurement technique. Since the accelerometers will be providing position information due to their orientation in a centrifugal field, sensing of steady coning angle on a rotor blade would require measurements down to zero (DC) frequency, thus, a large selection of piezoceramic accelerometers and piezo-film devices would not be applicable, due to their inability to measure constant accelerations (Ref. 61). This because these devices are charge-sensitive, and operate on the changing charge produced from strains in the piezoelectric component in the sensing unit. Since absolute charge in the device is not related to an applied acceleration level, the devices typically roll off at frequencies below 1 Hz.

Piezo-resistive accelerometers, and variable-capacitive accelerometers, are capable of measuring accelerations down to DC. The units used in the demonstration test, Entran EGA-125D (Ref. 62), use proof masses bonded to a piezoresistive beam that can sense steady deflections in a constant-g field. These units may be as small as 6mm x 3mm x 3mm and weigh less than a gram (without wires). Piezo-resistive devices typically produce millivolt-level outputs that require a differential amplifier prior to being used in an instrumentation system, and thus, the requirement for signal connections is equivalent to standard strain gauge bridges: two wires for excitation, two for the differential measurement, and possibly a third for a temperature compensation element. These same accelerometers were used in experiments on other model rotors, full-size wind tunnel tests, and flight tests on a highly instrumented helicopter (Refs. 28-35).

Variable capacitive accelerometers have recently become available as an alternative to piezo-resistive devices, and may be made in packages that are quite small since they are often manufactured from silicon using standard integrated-circuit techniques. Endevco Corporation (Ref. 61) manufactures the model 7290A Microtron accelerometer that is based upon this technology, and provides essentially *zero* drift in a 1in x 1in x 0.5in package weighing 9 grams. This particular device is currently being installed on the RASCAL UH-60A variable stability helicopter at NASA Ames Research Center (Ref. 50). Output signals are in the range of conventional data recording equipment (volts) and thus signal conditioning and wiring connections are minimized.

A related variable-capacitance device has been made available by Analog Devices, the ADXL50 accelerometer, that has been developed for use in automotive applications as an airbag triggering unit (Ref. . This sensor is provided in a TO-15 metal can, requires only a 5v supply, and has an output range of 2 volts covering a sensitivity of 50 "g" acceleration. It also includes a self-test feature for verification of sensor operation, and is very low cost, due to its high volume production. A sample of this unit has been obtained for bench testing to determine its DC drift performance over an extended operation. This device has been currently selected as the most likely candidate for inclusion in a prototype development program due to its small size, minimal electrical requirements, low cost, and strong performance.

5.2 Signal Conditioning and Scaling

Signal conditioning for the sensors to be used with this system would consist of either differential amplifiers, for the case of piezo-resistive accelerometers, or simple unity-gain buffer amplifiers for variable-capacitance accelerometers. As discussed previously, other potential means exist for rotor blade position measurements, but as these are not currently deemed viable alternatives to an all-accelerometer measurement scheme, discussion of signal conditioning for these units is unwarranted. Differential amplifiers are available as self-contained integrated circuits requiring only minimal external components, and some recent data acquisition modules actually provide differential amplification along with A/D conversion (Ref. 64, 65).

5.3 Signal Transmission and Telemetry

Signal transmission from a rotor blade to the rotorcraft fuselage and/or a ground station provides one of the more difficult challenges associated with production of a generic rotor motion and loads measurement device. While slipring technology has matured and has been used in past rotorcraft instrumentation efforts, a truly generic piece of rotor blade test instrumentation should provide both its own power and telemetry capability. Two obvious options thus exist to perform this telemetry function: RF and optical links.

Optical links typically require line-of-sight paths between the transmitter and receiver, except for operation in closed spaces (where reflected signals may be used), such as in typical hand-held IR remote controllers used in TV and audio components. Earlier IR units were limited to operation at frequencies of around 100KHz, but newer technologies and computer peripheral networking requirements have helped extend these devices to comply with the Infrared Data Association (IrDA) serial infrared standard (Ref. 66, 67). This specification calls for a maximum 1m range with transmission rates up to 115.2 Kbits/s over a viewing angle from $\pm 15^\circ$ to $\pm 30^\circ$. Power requirements for these units is modest, in order to accommodate the typically battery-based sources for laptop computers. While these are impressive specifications for an optical link "baud rate", the limited line of sight for operation would thus require a "ring" of transmitters located below the rotor blades so as to ensure that an emitter was always within view of a receiver as the rotor

system rotated around the shaft. An alternative to the "ring" approach would be a system that stored rotor motion and loads data in a buffer, and then transmitted the data in a "burst" when the rotor blade passed over the top of a fuselage-mounted detector. This scheme would thus update the estimates of rotor motion and loads at N/rev , where N is the number of rotor blades on the aircraft.

RF-based telemetry has been a staple of the flight test community for years. Recent advances in circuit subminiaturization, and expansion of wireless communication for everything from personal digital assistants and cellular telephones to computer peripherals, has brought the underlying technology into the hands of many. This has resulted in a wide array of potential telemetry systems, available at low cost, that would be acceptable for use in this application. An indication of where this technology may be headed appeared in Ref. 68, that described an effort by the Harris Corporation to develop subminiature instrumentation that integrates an antenna, sensors, processing chips, battery and adhesive backing. This so-called "peel-and-stick" instrumentation has obvious advantages of making extensive instrumentation of an aircraft much easier, in that each sensor is relatively autonomous, and would communicate with a central receiver using spread-spectrum RF links. These units are still in the research phase (Ref. 69), and have considerable capabilities above and beyond what would be required for this application (Ref. 70); as a consequence, their price reflects their custom nature.

A related technology, developed by BF Goodrich (Ref. 71), consists of sensors that report local stress levels in composite materials when interrogated by an RF source. This method of telemetry has also been suggested by researchers at the University of Michigan (Ref. 72), and is available in a related form as a commercial product to replace bar code reader devices (Ref. 73). This technology is still maturing, and suffers from the increased RF energy required to send out a signal and then interpret its return characteristics.

More traditional telemetry transceivers for short distance broadcasting have benefited from the reduced power requirements of surface-mount electronic packaging so as to provide secure operation, as well as avoid requirements for FCC operating licenses (Ref. 74-76). This is particularly true of many home audio-video products that have incorporated the new allocation of 900MHz-band of frequencies for short distance RF video and audio transmission (Ref. 77). Older applications have used conventional AM or FM bands at low power levels, since integrated circuits for constructing receivers for commercial radio are inexpensive and plentiful (Ref. 78). Some other units have used intermediate frequencies allocated for short-distance FM voice transmission or radio-controlled hobby applications near 40 MHz. Considerations for telemetry units are that the transmission frequency is approximately 10 to 20 times the data rate in order to assure reliable RF communication, and thus, broadcast on AM or intermediate FM radio links may not provide sufficient bandwidth for serial digital data PCM streams.

5.4 Signal Processing

Signal processing requirements of the instrumentation approach are to convert measured accelerations into estimates of rotor motion and loads during flight. These involve essential linear operations, with a "matrix inverse" handles as a linear combination of measurements from separate accelerometers that is used to drive an integration process. The output of the integration operation would be the rotor motion states, which in turn could be further transformed to represent spanwise loading information. Ideal operation would have these functions "hard-wired" into the measurement unit, but in actuality it is anticipated that some form of either reprogramming and/or mode selection would be required to accommodate the various hub geometries anticipated for the application of this

device. As was illustrated in the earlier sections of this report, this would be especially true for the case of flapping measurements on a semi-rigid (teetering) rotor system.

Microprocessors and single-board computers capable of performing this task come in a bewildering array of sizes, options and capabilities. For this instrumentation application, functionality associated with a programmable controller device appears to be most appropriate. For example, RISC-based miniaturized devices such as the BASIC Stamp (Ref. 79) provide limited computational capability, although incorporate the convenience of high-level programmability, simplified serial interfacing, and low power requirements; this unit would probably only be able to format limited bandwidth PCM streams, and not handle the full mathematical operations called for in a Kinematic Observer. Conventional microcontrollers, such as the 68HC11 (Ref. 80) or the Z180 (Ref. 81) would provide for sufficient computational power for data collection, processing, and transmission to a recording or other instrumentation system. While complete PC-compatible units are available in credit-card size formats (Refs. 82, 83), their generalized structure may make them overqualified for this application, but their ease of interfacing with conventional PCs would make software development border on the trivial. Selection of the most appropriate processor is left for the prototype development work that would be performed under a Phase-II continuation of this project.

5.5 Data Storage and Archiving

Storage of rotor motion and loads data could be performed in a fuselage-mounted unit that would possibly interface with other flight test hardware, but given the potential ranges of customer requirements on equipment for performing this task, this particular problem would not be provided as part of this instrumentation system.

5.6 Instrumentation Power Issues

If the instrumentation is to remain "autonomous", the data from the units would have to be telemetered, and the power would have to come from internal batteries. In order to assess the power requirements of this proposed measurement technique, an initial "cut" may be made by considering the power requirements of the sensors themselves. The ADXL50 accelerometer has a quiescent maximum power requirement of 65mW, which if added to an output power requirement of 4mW necessary to drive a 20K Ω load, yields a total requirement of 70mW. Assuming a nominal battery energy density of 10 W-hr/kg (NiCad batteries are typically 20), then the battery weight would be approximately 7gm/hour of operation. This of course does not include the power requirements for any signal processing, and so on, but this would probably involve a unit mounted significantly inboard, away from the actual accelerometer sensors. Reduced weight, at increased cost, may be possible using NiH batteries, as has been done in battery-powered satellite applications.

An alternate means of powering the sensors is to use rectified RF energy directed at these devices, as was done in Ref. 72, but this specialized device was located very close to the RF source and thus the power losses from this approach were minimal. RF energy pumped across lengths of a conventional rotor blade would be too troublesome to realistically use in this fashion.

5.7 Device Installation and Removal

Rapid installation and removal of this instrumentation would be ideal for use in a flight test program. In order to avoid specialized mechanical attachments, some form of

adhesive bond would be necessary between the instrumentation and the blade to be measured. To assess the requirements of the adhesive, one may again use some simple analysis as was done in the previous paragraphs. NiCad battery density is approximately 77 gm/cu in, or .17lbm/cu in. If a battery is restricted to a maximum height of 1/2 inch, then the applied stress from battery weight is .085lbm/sq in. If this battery is located at the blade tip, it would experience a 900g centrifugal load (for an SH-60 Seahawk), and thus require a shear stress of 77 psi to remain attached to the blade. Typical adhesives range from 100 psi to 5000 psi in shear strength, from rubber cement to CA glues. Thus, any high-strength adhesive would be suitable for attachment.

Removal of these devices would be accomplished either by chemically attacking the bonding agent, or through design of a "peel tab" into the instrument mounting attachment. Such a tab would allow conversion of the peel forces into tensile and tearing loads, which are known to be the weakest component of most adhesives. If the bonding agent and the bond are not readily removable, instead of sacrificing the instrumentation and destroying it during the removal process, one may use a "mounting pad", which would function as a low-cost expendable holster that provides interconnection of a removable battery and accelerometer sensor(s). Installation would thus involve attaching the entire device, whereas removal would first separate the expensive components from the mounting pad, and then scraping (destroying) the mounting pad off the surface of the blade. These mounting pads would most likely have a high aspect ratio (oriented spanwise) to ensure a satisfactory adhesive bond by minimizing blade aerodynamic curvature effects.

6.0 CONCLUSIONS FROM PHASE-I WORK

The overriding conclusion from this Phase-I effort is that the proposed instrumentation scheme, using a combination of blade-mounted accelerometers and a Kinematic Observer for signal processing, is indeed a viable means of acquiring rotor blade motion and loads data from a flight test program. Sensitivity studies using simulated blade response showed that the known difficulties inherent in this approach are surmountable, and that the system has added benefits over other distributed sensing schemes for rotor blade motion and loads measurement. Demonstration testing showed conclusively that blade-mounted accelerometers may be used to *replace* conventional instrumentation for measuring rotor response variables, through direct comparison with a flapping angle transducer mounted on a model rotor hub. And finally, implementation issues of data conversion, transmission, and sensor power and installation requirements can all be satisfactorily handled using conventional, "off the shelf" techniques. In short, the technique appears to be ready for initial prototyping work, as proposed for the Phase-II follow on work in the section that follows.

Because of the inherent flexibility of the proposed measurement technique, applications other than helicopter rotors may be possible. Given a compact and easy to install acceleration measurement unit, many problems of both rotating component balancing and load monitoring may be addressed. Machinery condition monitoring may be possible using these devices, where strain-gauge based instruments would be too difficult to properly attach to the rotating component.

Finally, detailed measurements of rotor blade motion and loads using this instrumentation would potentially allow for an improvement in the dynamic characteristics of helicopter and tiltrotor rotor systems. This could be achieved by providing information for flight control systems that may utilize rotor state feedback, which may allow for enhanced levels of agility to the pilot. This is, in fact, the purpose of the rotor mounted instrumentation on the UH-60 RASCAL aircraft at NASA Ames Research Center.

7.0 PHASE-I OPTION WORK PLAN

While implementation issues were addressed from a design standpoint, no experimental work was performed in the testing of any of the proposed techniques of Section 5. Thus, as part of the Phase-I Option associated with this work, some of these implementation issues would be addressed. These are briefly outlined below.

7.1 Hot-Bench Testing of System

Use of the accelerometers in the demonstration testing associated with this Phase-I effort did not incorporate individual signal conditioning and data conversion devices as would be associated with an autonomous, removable instrumentation system. Thus, it would be of interest to couple the proposed accelerometer units (currently the ADXL50 devices) with A/D converter units that would allow for the interconnection of several of these accelerometer sensing devices on a rotor blade. The experience gained from this "hot bench" testing of these electronic components would allow for direct, in-service assessment of their performance, power requirements, and handling and installation issues. This would comprise roughly half of the Phase-I Option work plan.

7.2 Telemetry and Power Conditioning Investigations

The second component of the Phase-I Option testing would include the design and development of a low-power telemetry unit, suitable for transmission from the rotor down to a fuselage-mounted data recording device. Power measurements under battery operation would aid the design of the units so as to assure that they remain operational throughout the anticipated lifetime associated with a flight test program. This may include designing battery replacement attachments that would allow for ready installation of fresh batteries on components that were to be left on an aircraft for an extended period of time. Bench testing of these devices, including a possible spin test of a telemetry transmitter, would comprise this component of the Option Task.

8.0 RECOMMENDATIONS FOR PHASE-II CONTINUATION

While several issues relating to the sensitivity of this measurement approach to sources of error have been addressed in this Phase-I study, most of the effort was concentrated on measurement of out-of-plane rotor motion and loads. A complete extension of the measurement methodology to in-plane and torsional response measurement was not performed, but would naturally follow from the work that was performed here. This would constitute part of the work that would be addressed in a Phase-II continuation of this device development. While a complete work statement for such an investigation is better left to a formal Phase-II proposal, this section will touch upon some general considerations that would be investigated in follow-on efforts.

8.1 Extensions to Simulation Analysis

The simulation developed for the sensitivity studies is sufficiently general in that an extension to completely handle in-plane and torsional rotor blade response for a variety of hubs would not be difficult, but should be performed in order to aid the development of a full-motion measurement device. This would allow for a realistic representation of all the coupling effects that may influence sensed acceleration at spanwise locations, providing additional help in the transitioning of this concept to a working prototype.

Since spanwise-mounted instrumentation would also be used for sensing in-plane and torsional motion, one of the goals of this extension would be to investigate the possibility of combining the required accelerometer configurations for this full-motion measurement to fixed spanwise stations. By combining instrumentation into a "cluster" at specific blade locations, issues related to signal transmission and instrument power would be simplified. This may even include having special "dies" developed, in conjunction with electronics manufacturers, that include multi-dimensional acceleration sensing and signal conditioning for this application.

8.2 Follow-On Demonstration Tests

Follow-on testing would be desirable to validate the method for measuring in-plane rotor response, torsional response, and higher modal response. Some of this validation may be possible through the continued use of the TRENDS UH-60 Airloads database, since the "strain gauge blade" had numerous strain gauges and accelerometers mounted on it and was used in a variety of flight conditions. All of these data have not been completely cataloged and validated, however, and so additional model testing would be required for some of this validation as well. This may be done by adding strain gauges to the model rotor already tested under Phase-I, or by upgrading the instrumentation system developed for the teetering rotor of Ref. 33 through the addition of measurement channels and strain gauge sensors. This latter approach provides an opportunity to test pre-prototype instrument concepts on a man-rated rotor system through towed autorotation tests.

8.3 Device Prototyping

Device prototyping would evolve under Phase-II through a structured development program, using results from the Phase-I option testing, and a series of subsystem tests that would provide milestones in the device development prior to installation on a rotorcraft. Consultation with the U.S. Navy sponsor would identify a rotor system suitable for testing under a Phase II program, and would also provide guidance on any flight qualification issues that must be addressed prior to installation on a fleet aircraft for flight test work.

9.0 REFERENCES

1. Carico, D. and Madey, S. L., Jr., "Dynamic Interface - Conventional Flight Testing Plus a New Analytical Approach", Proc. AHS Conf. on Helicopter Testing Technology, Williamsburg, VA, October 1984.
2. Wood, T. L., Ford, D. G., and Brigman, G. H., Maneuver Criteria Evaluation Program, USAAMRDL TR 74-32, May 1974, AD782209.
3. Heffley, R. K., Jewell, W. F., Lahman, J. M., and Van Winkle, R. A., "A Compilation and Analysis of Helicopter Handling Qualities Data," NASA CR 3144, August 1979.
4. Harrison, J. M., "An Integrated Approach to Effective Analytical Support of Helicopter Design and Development," Paper no. 52, Proc. of the Sixth European Rotorcraft Forum, September 1980.
5. Howlett, J. J., "UH-60A Black Hawk Engineering Simulation Program: Vol. 1 - Mathematical Model", NASA CR-166309, 1981.
6. Corliss, L., DuVal, R. W., Gillman, H., Huynh, L. C., "A Comparison of Real-Time Blade Element and Rotor-Map Helicopter Simulations Using Parallel Processing," Proc. 46th AHS Annual Forum, May 1990.
7. Bell Helicopter Company, "Measurement of Dynamic Air Loads on a Full-Scale Semi-Rigid Rotor," TCREC TR 62-42, 1962.
8. Scheiman, J., "A Tabulation of Helicopter Rotor-Blade Differential Pressures, Stresses, and Motions as Measured in Flight," NASA TM X-952, 1964.
9. Beno, E., "CH-53A Main Rotor and Stabilizer Vibratory Airloads and Forces," Dept. of the Navy, SER 611493, 1970.
10. Shockey, G. A., Cox, C. R., and Williamson, J. W., "AH-1G Helicopter Aerodynamics and Structural Loads Survey," USAAMRDL TR 76-39, February 1977.
11. Heffernan, R. and Gaubert, M., "Structural and Aerodynamic Loads and Performance Measurements of an SA 349/2 Helicopter with an Advanced Geometry Rotor," NASA TM 88370, November 1986.
12. Seto, E. I., "NASA/Army Blackhawk (UH-60) Rotor Project Plan," NASA Ames Research Center, March 1986.
13. McKillip, R. M., Jr., "Periodic Control of the Individual Blade Control Helicopter Rotor," Vertica, Vol. 9, no.2, pp. 199-225, 1985.
14. Ham, N. D., "A Simple System for Helicopter Individual Blade Control Using Modal Decomposition," Vertica, Vol. 4, no. 1, 1982.
15. Hooper, W. E., "The Vibratory Airloading of Helicopter Rotors," Vertica, Vol. 8, no. 2, pp. 73-92, 1984.
16. Bousman, W. G., "The Response of Helicopter Rotors to Vibratory Airloads," Journal of the American Helicopter Society, October 1990, pp. 53-62.
17. Kaletka, J., "BO-105 Identification Results," Paper no 9, Rotorcraft System Identification, AGARD LS-178, October 1991.
18. Briczinski, S. J., and Cooper, D. E., "Flight Investigation of Rotor/Vehicle State Feedback," NASA CR-132546, 1975.
19. DuVal, R. W., "Use of Multiblade Sensors for On-Line Rotor Tip-Path-Plane Estimation," Journal of the American Helicopter Society, October 1980.
20. Fuller, J. W., "Rotor State Estimation for Rotorcraft," Proc. AHS Specialist's Meeting on Helicopter Vibration, Hartford, CT, November 1981.
21. Walker, A. R., and Payen, D. B., "Experimental Application of Strain Pattern Analysis (SPA) - Wind Tunnel and Flight Test Results," Proc. 12th European Rotorcraft Forum, Paper no. 79, September 1986.

22. Snyder, W. J., Cross, J. L., and Kufeld, R., "NASA/Army Rotor System Flight Research Leading to the UH-60 Airloads Program," Innovations in Rotorcraft Test Technology, Proc. American Helicopter Society Tech. Specialists' Meeting, October 1990.
23. Gagnon, R., "Blade Motion Sensor System Calibration," Report no. SER-70486, Sikorsky Aircraft, October 1981.
24. Heffernan, R. M., Yamauchi, G. K., Gaubert, M., and Johnson, W., "Hub Loads Analysis of the SA 349/2 Helicopter," Proc. 14th European Rotorcraft Forum, Paper no. 50, September 1988.
25. Gunsallus, C. T., Pellum, W. L., and Flannelly, W. G., "Holometrics: An Information Transformation Methodology," Proc. 44th AHS Annual Forum, Washington, D.C., 1988.
26. Gustavson, B., Pellum, W. L. and Robeson, E., "Systematic Application of Holometric Synthesis for Cost-Effective Flight Load Monitoring," Proc. 49th AHS Annual Forum, St. Louis, MO, 1993.
27. McKillip, R. M., Jr., "Kinematic Observers for Active Control of Helicopter Rotor Vibration," Vertica, Vol. 12, no. 1/2, pp. 1-11, 1988.
28. McKillip, R. M., Jr., "Experimental Studies in System Identification of Helicopter Rotor Dynamics," Vertica, Vol. 12, no. 4, 1988.
29. McKillip, R. M., Jr., "Active Control Rotor Model Testing at Princeton's Rotorcraft Dynamics Laboratory," Proc. 2nd International Conference on Rotorcraft Modeling, College Park, MD, 1988.
30. Ham, N. D., and McKillip, R. M., Jr., "Research on Measurement and Control of Helicopter Rotor Response Using Blade-Mounted Accelerometers: 1990-1991," Proc. 17th European Rotorcraft Forum, Paper 91-77, September 1991.
31. Ham, N. D., and McKillip, R. M., Jr., "Research on Measurement and Control of Helicopter Rotor Response Using Blade-Mounted Accelerometers: 1991-1992," Proc. 18th European Rotorcraft Forum, Paper 91-77, September 1992.
32. Ham, N. D., Balough, D. L., and Talbot, P. D., "The Measurement and Control of Helicopter Blade Modal Response Using Blade-Mounted Accelerometers," Proc. 13th European Rotorcraft Forum, September, 1987.
33. McKillip, R. M., Jr., and Chih, M. H., "Instrumented Blade Experiments Using a Light Autogiro," Proc. 16th European Rotorcraft Forum, September 1990.
34. McKillip, R. M., Jr., Ham, N. D., and Balough, D. L., "Research on Measurement and Control of Helicopter Rotor Response Using Blade-Mounted Accelerometers: 1992-1993," Proc. 19th European Rotorcraft Forum, September 1993.
35. Ham, N. D., "Helicopter Individual Blade Control Research at M.I.T., 1977-1985," Vertica, Vol. 11, no. 1/2, 1987.
36. Knight, V. H., Haywood, W. S., Jr., and Williams, M. L., "A Rotor-Mounted Digital Instrumentation System for Helicopter Blade Flight Research Measurements," NASA TP 1146, April 1978.
37. Simms, D., and Butterfield, C., "A Low-Cost PC-Based Telemetry Data-Reduction System," Proc. 4th National Conv. on Microcomputer Applications in Energy, Tuscon, Arizona, April 1990 (SERI TP-257-3737).
38. Simms, D., and Cousineau, K., "An Advanced Data Acquisition System for Wind Energy Projects," Proc. American Wind Energy Association Windpower '92 Conference, Seattle, Washington, October 1992 (NREL TP-442-5102).
39. Gelb, A. Applied Optimal Estimation. M.I.T. Press, Cambridge, MA, 1980.
40. Ljung, L. and Soderstrom, T. Theory and Practice of Recursive Identification. M.I.T. Press, Cambridge, MA, 1983.
41. Ljung, L. System Identification: Theory for the User. Prentice-Hall, Englewood Cliffs, NJ, 1987.

42. Bielawa, R. Rotary Wing Structural Dynamics and Aeroelasticity. AIAA Education Series, AIAA, Washington, D.C., 1992.
43. Harris, F., "The Rotor Blade Flap Bending Problem - An Analytical Test Case," Journal of the AHS, October 1992, pp. 64-67.
44. Quackenbush, T. R., Wachspress, D. A., and Boschitsch, A. H., "Computation of Rotor Unsteady Airloads with a Constant Vorticity Contour Free Wake Model," AIAA Paper 91-3229, September 1991.
45. Houbolt, J. and Brooks, G., "Differential Equations of Motion for Combined Flapwise Bending, Chordwise Bending, and Torsion of Twisted Nonuniform Rotor Blades", NACA Report 1346, 1958.
46. Hodges, D. and Ormiston, R., "Nonlinear Equations for Bending of Rotating Beams with Application to Linear Flap-Lag Stability of Hingeless Rotors," NASA TM X-2770, 1972.
47. Johnson, W. Helicopter Theory. Princeton University Press, Princeton, New Jersey, 1980.
48. Bjorkman, W. S., and Bondi, M. J., "TRENDS: The Aeronautical Post-Test Database Management System," NASA TM 101025, January 1990.
49. Junkins, J., ed. Mechanics and Control of Large Flexible Structures. Progress in Astronautics and Aeronautics, Vol. 129, AIAA, Washington, D.C., 1990.
50. Fletcher, J., personal communication, NASA Ames Research Center, December 1994.
51. Parry, D., "Encouraging Innovation," Avionics, December 1994, p.58.
52. Walton, J., "An Investigation of the Feasibility of Using Video-Based Motion Measurement for Recovering Helicopter Blade Kinematics," Topic #92-018, Army SBIR Phase-I Awards Abstracts, August 1994, p.1.
53. HLC1295-001 Infared Sensor data sheet, Micro Switch Division, Honeywell Corporation, Freeport, Illinois, no date.
54. Polapulse User's Manual, Polaroid Corporation, Cambridge, Massachusetts, no date.
55. Model GP12 3-D Digitizers data sheet, Science Accessories Corp., Shelton, Connecticut, 1993.
56. Iovine, J. Step Into Virtual Reality. Blue Ridge Summit, PA: Windcrest/McGraw-Hill, 1995.
57. Cohen, C., "Attitude Determination Using GPS," Ph.D. Dissertation, Dept. of Aeronautics and Astronautics, Stanford University, December 1992
58. SP5000 Two-Axis Tilt Sensor data sheet, Spectron Glass and Electronics, Inc., Hauppauge, New York, no date.
59. GyroChip™ product literature, Systrand Donner Inertial Division, Concord, California, no date.
60. Gyrostar™ catalog G-09-A, Murata Electronics North America, Smyrna, Georgia, 1993.
61. Endevco Standart Piezoelectric and Isotron Accelerometer catalog, Endevco Corp., San Juan Capistrano, California, April 1992.
62. Accerometer Instruction & Selection Manual, Entran Devices, Inc., Fairfield, New Jersey, 1983.
63. ADXL50 Accelerometer Specification Sheet, Analog Devices, Inc., Norwood, Massachusetts, 1994.
64. AD1B60 Intelligent Digitizing Signal Conditioner, Analog Devices, Inc., Norwood, Massachusetts, 1994.
65. LM12434 12 Bit + Sign Data Acquisition System with Serial I/O and Self-Calibration, National Semiconductor Corp., Santa Clara, California, 1994.
66. IrDA Transciever Module, Hewlett-Packard Company, Santa Clara, California, 1994.

67. SIRComm2 Serial IR Communications Receiver, Irvine Sensors Corp., Costa Mesa, California, 1994.
68. "Avionics Applications," Aviation Week and Space Technology, May 31, 1993, p. 42.
69. Mestas, V., Harris Corporation, personal communication, 1995.
70. "Subminiature Telemetry," Commerce Business Daily, PSA-1026, February 3, 1994, p.2.
71. "Remotely Interrogated Sensor Electronics," by BF Goodrich Aerospace, Vergennes, Vermont, in NASA Tech Briefs, January 1995.
72. Akin, T., Ziaie, B., and Najafi, K., "RF Telemetry Powering and Control of Hermetically Sealed Integrated Sensors and Actuators," IEEE Solid State Sensors and Actuator Workshop, Hilton Head, South Carolina, 1990, pp. 145-149.
73. M3394B ASIC Reader Chip, Diester Electronics USA, Inc., Manassas, Virginia, 1995.
74. 2000 Spread Spectrum Burst Processor, Zilog, Inc., Campbell, California, 1994.
75. 900 MHz CSMA Transceiver, Xetron Corp., Cincinnati, Ohio, 1994.
76. Micro-SAW Radio Transceiver, Hand Held Products, Inc., Charlotte, North Carolina, 1994.
77. Radio Shack 1995 Catalog, Tandy Corporation, Texas, 1995.
78. F-1001 Telemetry Transmitter, Binsfeld Engineering, Inc., Maple City, Michigan, 1992.
79. BASIC Stamp Development Kit, Parallax, Inc.
80. 68HC11 Evaluation Kit, Motorola Advanced Microcontroller Division, Austin, Texas, 1990.
81. Little Star, Z-world Engineering, Davis California, 1994.
82. Cardio-X86, Epson America, Inc., Torrance, California, 1994.
83. GCAT-6000 Single-Board Computer, The Saelig Company, Victor, New York, 1994.